Studies of Decay Schemes in the Osmium-Iridium Region. III. Decay of 15.8-Hour Ir^{186}†

G. T. Emery, W. R. Kane, M. McKeown, M. L. Perlman, and G. Scharff-Goldhaber
Brookhaven National Laboratory, Upton, New York

(Received 8 November 1962; revised manuscript received 13 December 1962)

The decay of 15.8-h Ir^{186} was studied with a double-focusing electron spectrometer, a lens spectrometer, and scintillation spectrometers. Several coincidence experiments were also performed. About two-thirds of the 101 transitions observed could be fitted into a level scheme for Os^{186} consisting of a ground-state ($K=0$) band, a $K=2$ (gamma-vibrational) band, and several other levels. The positron spectrum shows at least two branches; the branch with the highest end-point energy (1.94 ± 0.02 MeV) populates the $I=6$, $K=0$, state at 0.869 MeV. The total positron intensity is $(2.5\pm0.7)\%$. The most probable spin assignment for Ir^{186} (15.8-h) is 7. Energies of the collective levels of Os^{186}, and relative transition probabilities, are discussed in the framework of the existing knowledge of other even-A osmium isotopes, and are compared with the predictions of the band-mixed strong coupling model and of various versions of the asymmetric rotor model. An appendix gives data accumulated during the course of this work on transitions following the decay of Ir^{185} and of Ir^{187}.

I.

A. INTRODUCTION

THE even-mass isotopes of osmium have particular relevance to theories of nuclear structure because of the position they occupy in the transition region between the highly deformed nuclei and the spherical nuclei.[1] Furthermore, the energy levels of Os^{190} have been found to have properties[2] which are rather well described by the asymmetric rotor model of Davydov and Filippov,[3,4] in which it is assumed that the nucleus has the shape of a triaxial ellipsoid, i.e., that it has an equilibrium gamma deformation. It is promising, therefore, to investigate the decay of Ir^{186} to Os^{186}, for Ir^{186} has a large disintegration energy (3.81 MeV) and a high spin,[5] so that it appears possible to establish the properties of a large number of states of Os^{186} with various spins by this means. The information available from the decay of Re^{186} and of Ir^{186} before the present work began is summarized in Sec. IB. The early work on Ir^{186} was largely carried out at this Laboratory but has been published only in the Proceedings of the Pittsburgh Meeting (1957) and in private communications to Nuclear Data Sheets.

The internal conversion-electron spectrum emitted in the decay of 16-h Ir^{186} has been studied with a double-focusing 50-cm radius beta-ray spectrometer. This work is described in Sec. II A; in Sec. II B the following results are presented: the gamma-ray singles and coincidence spectra from this source as observed with NaI(Tl) scintillation spectrometers; the spectrum of high-energy gamma rays measured with a three-crystal pair spectrometer; and finally, data on electron-electron coincidences, on electron–gamma-ray coincidences, and on the positron spectrum of Ir^{186}, all of which were obtained with a magnetic lens coincidence spectrometer.

One hundred and one electromagnetic transitions in Os^{186} have been established and partially fitted into a scheme of 23 energy levels (Secs. III A, B, and C). These include a ground-state rotational band and another even parity ($K=2$) band, but the level characteristics deviate appreciably from those found in the strong coupling region.

The level scheme of Os^{186} is compared with the level schemes of other even-A Os isotopes, and the characteristic features of all these level schemes are pointed out in Sec. IV. In the same section the energies of the levels in Os^{186} and the transition probabilities between these levels are compared with the predictions from various nuclear models. Also in Sec. IV the present information on the spins of the even-mass Ir and Re nuclei and on the disintegration energies between the ground states of the even-A Ir and Os isotopes is discussed.

Appendix I contains information on the transitions following the decay of Ir^{185} and of Ir^{187}; these results are a by-product of the study of Ir^{186}. Arguments in support of the reliability of the level scheme adopted for Os^{186} are presented in Appendix II.

B. PREVIOUS WORK

1. Decay of Re^{186}

The beta decay of 88.9-h[6] Re^{186} populates levels in Os^{186} at 137 keV[7,8] and 768 keV.[9,10]

† Work performed under the auspices of the U. S. Atomic Energy Commission.

[1] G. Scharff-Goldhaber, in *Proceedings of the University of Pittsburgh Conference on Nuclear Structure, 1957* (University of Pittsburgh and Office of Ordnance Research, U. S. Army, 1957).

[2] W. R. Kane, G. T. Emery, G. Scharff-Goldhaber, and M. McKeown, Phys. Rev. **119**, 1953 (1960).

[3] A. S. Davydov and C. F. Filippov, Nucl. Phys. **8**, 237 (1958).

[4] A. S. Davydov and V. S. Rostovsky, Nucl. Phys. **12**, 58 (1959).

[5] This value for the decay energy was cited in a note added in proof to reference 2 (p. 1965). The direct positron connection to the 6+ level at 0.87 MeV implies a high spin for Ir^{186}.

[6] F. T. Porter, M. S. Freedman, T. B. Novey, and F. Wagner, Jr., Phys. Rev. **103**, 921 (1956).

[7] L. A. Beach, C. L. Peacock, and R. G. Wilkinson, Phys. Rev. **76**, 1585 (1949).

[8] R. M. Steffen, Phys. Rev. **82**, 827 (1951).

[9] F. R. Metzger and R. D. Hill, Phys. Rev. **82**, 646 (1951).

[10] M. W. Johns, C. C. McMullen, I. R. Williams, and S. V. Nablo, Can. J. Phys. **34**, 69 (1956).

The 137-keV level decays via an $E2$ transition.[8–10] It has also been reached by Coulomb excitation.[11] The reported values for the lifetime of this state are listed in Table I. The energy of this level and the enhancement

TABLE I. Measurements of the lifetime of the first excited state of Os^{186}. The measurement of Rester *et al.* was by observation of the yield of internal conversion electrons in Coulomb excitation; the remainder were delayed-coincidence measurements.

Author	Half-life (sec)	$\|M\|^2$
McGowan[a]	$(8 \pm 1) \times 10^{-10}$	102[f]
Berlovich[b]	$(6.0 \pm 0.2) \times 10^{-10}$	137
Rester *et al.*[c]	$(5.9 \pm 1.5) \times 10^{-10}$	139
Bodenstedt *et al.*[d]	$(8.4 \pm 0.3) \times 10^{-10}$	98
Bashandy and El Nesr[e]	$(8.7 \pm 0.4) \times 10^{-10}$	95

[a] F. K. McGowan, Phys. Rev. **81**, 1066 (1951).
[b] E. E. Berlovich, Zh. Eksperim. i Teor. Fiz. **33**, 1522 (1957) [Translation: Soviet Phys.—JETP **6**, 1176 (1958)].
[c] Reference 11.
[d] Reference 16.
[e] E. Bashandy and M. El Nesr, Nucl. Phys. **34**, 483 (1962).
[f] In the calculation of $|M|^2$ the nuclear radius parameter was taken to be 1.20×10^{-13} cm.

$|M|^2$ of the $E2$ transition to the ground state fit well into the regularities observed in the first 2+ states of even-even nuclei in this region.[1]

The 768-keV level decays via a direct ground-state transition and via a 631-keV cascade transition to the 137-keV level.[6,9,10] Several investigations of the angular correlation of the 631- and 137-keV gamma rays show that the spin of the 768-keV level is 2.[12] The parity of this state is even, because the beta branch from the 1- ground state of Re^{186} which populates the 768-keV state is first forbidden as shown by its logft value of 9.6 Increasingly smaller upper limits have been set on the relative intensity of a possible $M1$ component of the 631-keV transition[13–16]; the latest limit is 0.1% of the $E2$ component.[16] The spin of this level and systematics suggest that it is the lowest member of the gamma-vibrational ($K=2$) band.

2. Decay of Ir^{186}

Chu, in 1950, produced an 11.8-h iridium activity[17] by bombarding Re enriched in Re^{185} with 32-MeV α particles, and assigned it to Ir^{187}. Smith and Hollander[18] bombarded Ir with 120-MeV protons and obtained an ~2.5-h Pt activity with a 14-h Ir daughter, in addition to several other activities. They correctly assumed that the 14-h daughter was identical with the Ir activity found by Chu and concluded that its mass number must be 186 or 187. They preferred 187 because the gamma-ray spectrum from the 14-h Ir was different from that of Re^{186}: they had observed gamma rays emitted from this iridium activity with energies of 135±10, 300±10, and 435±15 keV, with relative intensities 1:1.1:0.8, respectively.

Consideration of regularities in the level patterns of even-A osmium nuclei led Scharff-Goldhaber[1] to suggest that the 435-, 300-, and 135-keV gamma rays may be due to transitions between the levels of a ground-state rotational band (6+ → 4+ → 2+ → 0+) in Os^{186}, the "135-keV transition" being identical with the 137-keV 2+ → 0+ transition found in the decay of Re^{186}. The difference between the spectra of Re^{186} and Ir^{186} was attributed to the fact that the spin of Ir^{186} must be high, while that of Re^{186} was known to be 1.[6] It was then shown that the three gamma rays of 435, 300, and 135 keV are indeed in cascade.[19]

Further study of the gamma-ray spectrum yielded transitions with the following energies and relative intensities: 137 (100), 297 (91.5), 434 (52.5), 625 (40.5), 773 (31.2) and 923 (~6) keV.[19] The first three transitions were shown to be $E2$ from measured K/L internal conversion-electron ratios.[20]

The internal conversion-electron spectra of Ir^{185}, Ir^{186}, and Ir^{187} were investigated with permanent magnet spectrographs by Diamond and Hollander.[21] They assigned six electromagnetic transitions to Ir^{186}; for twelve other transitions which might have originated from Ir^{186}, the possibility that they originated in Ir^{185} or Ir^{187} was not excluded.

The positron spectrum of Ir^{186} was measured by Alburger *et al.*[20] by means of an intermediate image spectrometer. An end-point energy of 1.92±0.05 MeV was obtained. Some indication of a lower energy positron branch was observed. The intensity of the positrons was found to be ~5% of the total decays.

II.

A. INTERNAL CONVERSION-ELECTRON SPECTRA

1. Double-Focusing Spectrometer and Its Calibration

Measurements of the internal-conversion electron spectra, upon which much of the finally deduced decay scheme depends, were made with a 50-cm radius, $\pi\sqrt{2}$, double-focusing spectrometer. The main magnet, vacuum chamber, and rotating coil system of this instrument, which were made at the Institute of Physics,

[11] D. H. Rester, M. S. Moore, F. E. Durham, and C. M. Class, Nucl. Phys. **22**, 104 (1961).
[12] J. P. Hurley and P. S. Jastram, Phys. Rev. **95**, 627 (1954).
[13] T. Lindqvist and I. Marklund, Nucl. Phys. **4**, 189 (1957).
[14] W. J. King and M. W. Johns, Can. J. Phys. **37**, 755 (1959).
[15] C. A. Lerjefors, E. Matthias, and E. Karlsson, Nucl. Phys. **25**, 404 (1961).
[16] E. Bodenstedt, H.-J. Körner, G. Strube, G. Günther, J. Radeloff, and E. Gerdau, Z. Physik **163**, 1 (1961).
[17] T. C. Chu, Phys. Rev. **79**, 582 (1950).
[18] W. G. Smith and J. M. Hollander, Phys. Rev. **98**, 1258 (1955).
[19] G. Scharff-Goldhaber, L. Grodzins, M. McKeown, and J. Hudis, private communication to *Nuclear Data Sheets*, National Academy of Sciences, National Research Council (U. S. Government Printing Office, Washington 25, D. C., 1959).
[20] D. E. Alburger, G. Scharff-Goldhaber, M. McKeown, and J. Hudis, private communication to *Nuclear Data Sheets*, National Academy of Sciences, National Research Council (U. S. Government Printing Office, Washington 25, D. C.).
[21] R. M. Diamond and J. M. Hollander, Nucl. Phys. **8**, 143 (1958).

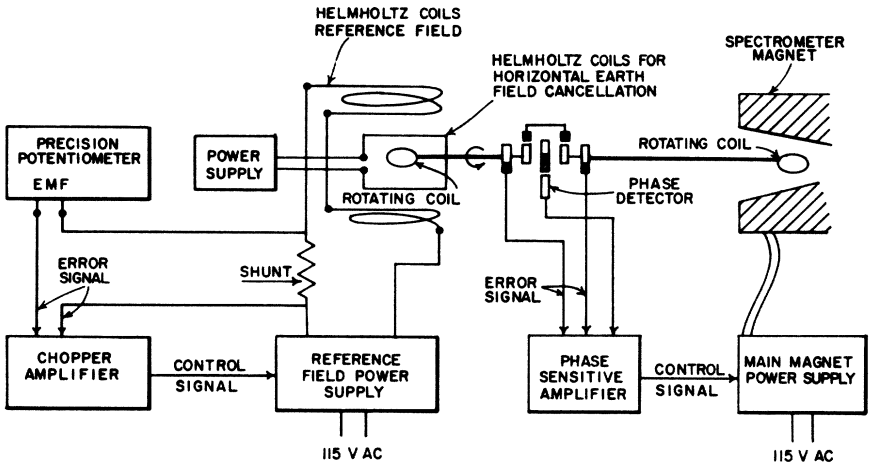

FIG. 1. Diagram of system for measurement and control of the magnetic field in the 50-cm double-focusing spectrometer.

Uppsala,[22] have been described.[23] As is the case with other spectrometers of this design, the field strength in the iron analyzing electromagnet is measured by comparison with another field produced by Helmholtz coils, both fields being sensed by small rotating coils, one at each end of a long shaft. In the BNL spectrometer, power for the two magnets is supplied by transistorized, servocontrolled rectifiers from the 60-cycle ac lines. A block diagram of the power supply and field measurement system is shown in Fig. 1. The Helmholtz reference-field coils and the rotating coils are cooled by oil maintained at constant temperature. A Leeds and Northrup Wenner potentiometer, accurate to 0.01%, serves to control the entire system and gives a linear measure of electron momentum. The Helmholtz reference-field current is automatically held at the value which produces a null between the potentiometer voltage and the voltage developed at a precision shunt in series with the Helmholtz coil. The current in the main magnet coil is controlled by a second power supply so as to produce a null in the signal representing the difference between the voltages generated in the two rotating coils, one in the reference field and the other in the spectrometer field. A small Helmholtz coil is used to cancel the horizontal component of the earth's field at the position of the reference field; the vertical component is a linear addition to the vertical reference field. Thus the potentiometer voltage V and the spectrometer field B are related by the expression

$$B\rho = k(V - V_E), \tag{1}$$

where V_E is the voltage necessary to compensate for the vertical component of the earth's field in the reference coil, and ρ is the orbit radius.

A cylindrical proportional counter with methane flow at 10 cm pressure was used as the detector in these measurements. Electrons entered the active region through a side window consisting of aluminized Mylar which had been lightly coated on the outer side to seal pinholes; the total surface density was 1.00 mg/cm^2.

Momentum linearity and transmission characteristics of the spectrometer were tested with sources of ThB and its daughter products electrostatically deposited from decaying thoron onto narrow aluminum strips. As shown in Table II, the measured $B\rho$ values of the E, F, L, and P lines relative to that for the I line agree with values taken from the literature[24] well within the estimated uncertainties, about 2 to 3 parts in 10^4. The B line appears to have been slightly degraded by an amount which would correspond to a source thickness of a few micrograms per cm^2. Within much larger uncertainties the integrated line intensity ratios, also, agree well with published results.[24] The B-line intensity was corrected

TABLE II. Momenta and intensities of electron lines from ThB and its daughters. Values measured with the 50-cm spectrometer and values from the literature are given.

Line	Energy	$H\rho/H\rho$(I-line) Measured	$H\rho/H\rho$(I-line) Literature[c]	Intensity Measured	Intensity Literature
B	36.2	0.37135(16)	0.37198(4)	4.7[a]	4.7
E	98.8	0.63267(22)	0.63273(13)	0.40	0.47
F	148.1	0.79152(15)	0.79161(10)	28	28[b]
I	222.2	1.00000	1.00000	5.0	4.7
L	422.8	1.48644(30)	1.48639(20)	0.63	0.67
P	772.5	2.23989(50)	2.23915(45)	0.09	0.11

[a] This value has been corrected for counter window transmission. The uncorrected value is 3.3. For lines other than the B line corrections are negligible.
[b] Measured intensities have been normalized at the value for the F line.
[c] Cf. reference 24.

[22] We are indebted to various staff members of the Institute of Physics and especially to Dr. Torsten Lindqvist for the construction of these major parts of the spectrometer, and we wish to express our appreciation to them.

[23] A. Hedgran, K. Siegbahn, and N. Svartholm, Proc. Phys. Soc. (London) **A63**, 960 (1950); G. Bäckström, Nucl. Instr. **1**, 253 (1957).

[24] K. Siegbahn and K. Edvardson, Nuclear Phys. **1**, 137 (1956); G. Lindstrom, Ark. Fysik 4, 1 (1952); C. de Vries, Nucl. Phys. **18**, 428 (1960); A. I. Zhernovoy, E. M. Krisyouk, G. D. Latyshev, A. S. Remenny, A. G. Sergeyev, and V. I. Fadeyev, Zh. Eksperim. i Teor. Fiz. **32**, 682 (1957) [translation: Soviet Phys.—JETP **5**, 563 (1958)]; V. D. Vorobyov, K. I. Ilyn, T. I. Kolchinskaya, G. D. Latyshev, A. G. Sergeyev, Yu. N. Trofimov, and V. I. Fadeyev,

for the 70% counter window transmission[25]; the L and P intensities are expected to be somewhat low because of recoil loss of ThC″.

2. Source Preparation and Internal Conversion-Electron Measurements

Ir^{186} sources were prepared by bombardment of rhenium, enriched[26] to 96% in Re^{185}, with alpha particles in the Brookhaven 60-in. cyclotron. The relatively weak sources needed for positron and gamma-ray spectroscopy and for the coincidence work were prepared from rhenium irradiated in the external beam. The intense irradiations required to prepare sources for internal conversion spectroscopy were carried out in the internal beam. For these irradiations about 25 mg of enriched rhenium metal was electroplated onto the face of a gold receiver. This deposit, about one cm^2 in area, was then heated in a hydrogen atmosphere to sinter it. The irradiations lasted 12 to 15 h at a current of $\sim 40\ \mu A$; the gold was internally water cooled. After irradiation the rhenium was dissolved in concentrated nitric acid, about $20\ \mu g$ of inactive iridium carrier and a little sulfuric acid were added, and the solution was heated to volatilize the Re_2O_7. Removal of the rhenium was made essentially complete by repeated addition of nitric acid to the heated sulfuric acid solution. Finally, the small amount of remaining material was dried and dissolved in a small volume of NH_4HSO_4 (pH 3.6); then the iridium was electroplated onto a thin gold foil in a rectangular area 3 mm×20 mm. The disintegration rate of the strongest source prepared was about 10^8/sec.

Although the activity in these sources was mostly that of Ir^{186}, relatively small amounts of Ir^{185}, Ir^{187}, and Ir^{188} were also present. No special difficulty was caused by Ir^{188}; its radiations have been identified,[21,27–29] and its 41-h half-life allows it to be distinguished from Ir^{186}. Differentiation by decay among Ir^{185}, Ir^{186}, and Ir^{187}—whose half-lives have been reported as 15±3 h,[21] 15±2 h,[19,21] and 11.8±0.3 h,[17,21] respectively—was in most cases impractical. In the conversion-electron spectroscopy this differentiation was made by comparison of two sources produced by irradiation of Re^{185} with alpha particles, one at an energy of 40 MeV and the other at 34 MeV. A small part of the spectrum from each of the sources is shown in Fig. 2; the ordinate of the curve for the 40-MeV irradiation has been normalized by fitting at a well-known Ir^{186} line, K 297 keV. It is clear that the effect of the decrease in alpha-particle energy was to lower the line intensities of Ir^{185}, produced by the $(\alpha,4n)$ process, and to raise those of Ir^{187}, produced by the $(\alpha,2n)$ process, with respect to the intensities of Ir^{186}, the $(\alpha,3n)$ reaction product. With few exceptions it was thus possible to give isotopic assignments to the 235 observed electron lines.

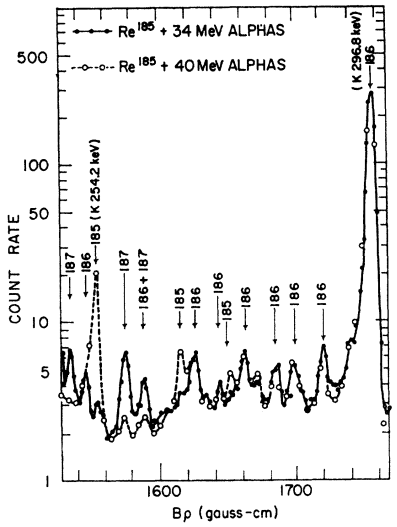

FIG. 2. Parts of the conversion-electron spectra of two iridium sources prepared from Re^{185} irradiated with alpha particles. Assignment of lines to the several isotopes indicated by mass number was made possible by the variation produced in their relative abundances by change of bombardment energy. Intensities are normalized at the line K 296.8 keV.

Decay data obtained for some lines confirm their assignments; and from some of these data the half-life information shown in Table III has been obtained; it is more accurate than that available until now.

TABLE III. Half-lives of Ir^{185}, Ir^{186}, and Ir^{187} obtained from internal conversion-electron intensity measurements.

	Conversion line (keV)	Half-life (h)
Ir^{185}	K 254.16±0.11	14.2±1.0
	K 489.05±0.20	13.8±1.4
		Av=14.0±0.9
Ir^{186}	K 137.15±0.03	15.8±0.3
Ir^{187}	L_3 65.15±0.05	10.5±0.3

Line intensities generally were taken from peak-height values after subtraction of background estimated from the shape of the adjacent parts of the spectrum. The more carefully scanned spectrum from the source prepared at 34 MeV was used. The peak-height values were then corrected for decay and for line broadening caused by source thickness. A curve representing the

Izvestia Akad. Nauk SSSR, Ser. Fiz. **21**, 954 (1957) [translation: Bull. Acad. Sci. USSR **21**, 956 (1957)]; E. M. Krisyouk, A. D. Vitmen, V. D. Vorobyov, G. D. Latyshev, and A. D. Sergeyev, Izvestia Akad. Nauk SSSR, Ser. Fiz. **20**, 877 (1956) [translation: Bull. Acad. Sci. USSR **20**, 797 (1956)].

[25] R. Arnoult, Ann. Phys. **12**, 241 (1939); see also H. Slätis, in *Beta- and Gamma-Ray Spectroscopy*, edited by Kai Siegbahn (North-Holland Publishing Company, Amsterdam, 1955), p. 269.

[26] This material, consisting of 96% Re^{185} and 4% Re^{187}, was supplied by the Y-12 Plant, Union Carbide and Carbon Corporation, through the Isotopes Division, U. S. Atomic Energy Commission, Oak Ridge, Tennessee.

[27] P. S. Fisher and R. A. Naumann, Phys. Rev. **112**, 1717 (1958).

[28] Walter R. Kane, thesis, Harvard University, December 1958 (unpublished).

[29] R. L. Graham, J. S. Geiger, R. A. Naumann, and J. M. Prospero, Can. J. Phys. **40**, 296 (1962).

broadening correction factor was derived from the shapes of eight well resolved K lines distributed over the spectrum; values for this factor at electron energies 45, 250, and 350 keV are 2.6, 1.10, and 1.03, respectively. Corrections for counter-window absorption are negligible.

Both spectra were measured at an instrumental resolution of ~0.30%, full width at half-maximum. Comparison of lines which were scanned in detail showed that there was no detectable spectrometer calibration shift between the two sets of measurements. From measurements of the F and L lines of a ThB source the spectrometer calibration constant k, Eq. (1), was determined to be $(8.6058\pm0.0017)\times10^{-3}$ G-cm/μV. The momenta of the two reference lines were taken to be 1388.44±0.10 G-cm and 2607.17±0.30 G-cm, respectively. Some checks on the calibration are presented in Table IV: for a few of the prominent transitions in Os^{186}, energy values computed from several internal conversion lines are shown.

From the potentiometer readings corresponding to the peak positions of the lines, electron energies and possible transition energies corresponding to conversion in the K, L, and M shells[30] were calculated by IBM 610 computer. Uncertainties associated with these values were derived from the estimated limits of uncertainty in peak positions and from the calibration error. Actual transition energies were then extracted from this compendium by the usual search method.

An example of several transitions which are observed as one peak in the scintillation spectrum but which were clearly separated in the conversion spectra is shown in Fig. 3.

In Table V are shown the properties of the 101 transitions thus found in Os^{186}. Each has been classified according to a "level of confidence": transitions in group A have been observed as two or more well-defined electron lines whose energies are related accurately by binding energy differences; all other electron lines from these transitions have been accounted for. Group C transitions are usually represented by one line, sometimes weak or broad; these have often been identified as K lines by a process of elimination. The transitions in group B are intermediate in reliability.

The level scheme finally deduced for Os^{186} is based to a large extent on the analysis of the conversion-electron spectra. Coincidence data and information from the positron and gamma-ray "singles" measurements were

TABLE IV. Energies of three $E2$ transitions in Os^{186}.

Approx. energy (keV)	Conversion line	Transition energy[a] (keV)	Weighted mean energy (keV)
137	K	137.02 ±0.03 (137.144±0.03)	
	L_2	137.03 ±0.07 (137.149±0.03)	
	L_3	137.05 ±0.08 (137.144±0.03)	137.040±0.038 (137.146±0.030)[c]
	$M_{2,3}$	137.10 ±0.16[b]	
	N	137.06 ±0.17[b]	
297	K	296.76 ±0.08	
	$L_{1,2}$	296.78 ±0.12[b]	
	L_3	296.78 ±0.17	296.75 ±0.06
	M	296.61 ±0.14[b]	
	N	296.85 ±0.19[b]	
434	K	434.83 ±0.14	
	$L_{1,2}$	434.80 ±0.16[b]	434.78 ±0.08
	M	434.82 ±0.17[b]	
	N	434.63 ±0.22[b]	

[a] Atomic electron binding energies were taken from reference 30.

[b] A weighted average of the subshell binding energies was used.

[c] The values given in parentheses were derived from measurements with a $Re^{186+188}$ source which was thinner than the Ir sources. The 155-keV transition in Os^{188} was used as an internal calibration standard. The energy of this transition, recently measured with a bent-crystal spectrometer by B. Lindström and I. Marklund [Ark. Fys. **22**, 422 (1962)], and with an iron-free double focusing spectrometer by Graham, Geiger, Naumann, and Prospero (reference 29), was taken to be 155.032±0.012 keV from the two respective results (155.032±0.012) keV and (155.03±0.03) keV. The value (137.146±0.030 keV) thus obtained is considered to be more accurate than the value obtained at a lower resolution with the thicker Ir^{186} sources, and was therefore adopted in this paper. It agrees well with the values (137.157 ±0.008 keV) found by Lindström and Marklund and (137.19±0.07 keV) obtained with a magnetic-lens spectrometer by Porter *et al.* (reference 6), and disagrees only slightly with the value (137.22±0.03 keV) obtained with a bent-crystal spectrometer by N. Ryde and B. Andersson [Proc. Phys. Soc. (London) **B68**, 1117 (1955)]; all three values were obtained with Re^{186} sources. It is believed that our values for the higher energy lines were not appreciably affected by the thickness of the iridium sources.

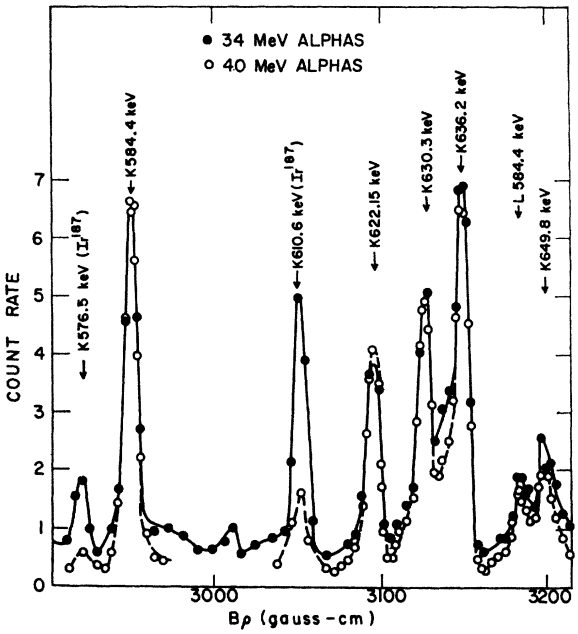

FIG. 3. Parts of the conversion-electron spectra of two iridium sources, showing the resolution of several important transitions. The method of isotope assignment is the same as that shown in Fig. 2. Intensities are normalized at the line K636.2 keV.

[30] Atomic electron binding energies have been taken from the data of Cauchois, quoted in *Nuclear Spectroscopy Tables*, edited by A. H. Wapstra, G. J. Nijgh, and R. van Lieshout (North-Holland Publishing Company, Amsterdam, 1959).

TABLE V. Transitions observed in the decay of Ir^{186}. Column (1) gives the designations (cf. Figs. 5, 6) of the two levels directly connected by the transition whose energy is given in column (2). Energy values marked by an asterisk were used in the least-squares evaluation of the level energies. Intensities of column (3) refer to K lines except where otherwise indicated, and $1.2(-1)$ is to be read as 1.2×10^{-1}; observed peak counting rates were approximately 10^5/min multiplied by the number given. In column (4), $L_{1,2}$ designates an unresolved pair of lines as distinct from L_1, L_2. The significance of column (5) is given in the text, in Sec. II. A.2. The relative transition intensities of column (6) are based on the observed conversion-line intensities and theoretical conversion coefficients (reference 33) unless other information is given in column (4). In those cases where no multipole assignments could be made, two intensities are given as probable limits; these have been calculated from $E1$ and $M1$ conversion coefficients. An intensity of 25 represents approximately 100% of the Ir^{186} decays. Multipole orders given in parentheses should be regarded with caution. The uncertainties in column (2) are derived from the statistical uncertainties in the line positions and the uncertainties in the calibration line energies. Systematic errors are expected to be small, but are not included. For the measurement of the energy of the 137-keV transition, see footnote c to Table IV.

(1) Designation	(2) E_γ (keV)	(3) Conversion line intensity	(4) Conversion lines observed, basis of multipole assignment, remarks	(5) Class	(6) Multipole assignment; transition intensity (25≅100% of Ir^{186} transitions)	
VU	70.88±0.20*	$1.2(-1)L_1$	L_1, L_2, L_3. M hidden. $L_1/L_2=2.5\pm1.3$; $L_1/L_3=1.4\pm0.5$.	A	$E1$	1.8(0)
	87.19±0.20	$2.6(-2)L_3$	$L_{1,2}$, L_3. $L_2/L_3<2.3$.	C	($E2$)	$8.2(-2)$
	102.12±0.20	$2.4(-2)L_2$	L_2, L_3, M? $L_2/L_3=1.2\pm0.3$.	C	$E2$	$8.2(-2)$
	119.36±0.20	$6.1(-2)$	K, L_1?, M?	C		$[9.1(-2)<I<2.2(-1)]$
BA	137.15±0.03*	4.6(0)	K, L_2, L_3, M, N. $K/L_2/L_3/M/N=(4.6\pm0.4)/(3.6\pm0.2)/(2.7\pm0.1)/(1.3\pm0.05)/(0.3\pm0.03)$.	A	$E2$	2.3(+1)
GF	143.00±0.20*	$1.0(-1)$	K, L_2, M. L_3 hidden. $K/L_2/M=(1.0\pm0.1)/(0.3\pm0.03)/(0.7\pm0.3)$.	A	$0.7E2$, $0.3M1$	$3.4(-1)$
HG	160.02±0.20*	$2.1(-2)$	K. L_2, L_3 hidden? Decay scheme.	C	($E2$)	$1.3(-1)$
	167.05±0.20	$1.3(-2)$	K. L's hidden?	C		$[2.7(-2)<I<1.7(-1)]$
	219.96±0.15	$1.7(-2)$	K, L_2. L_3 hidden. $K/L_2=2.3\pm0.7$.	B	$E2$	$1.6(-1)$
	224.13±0.16	$1.9(-2)$	K, L_1. $K/L_1=7.4\pm3.2$.	B	$M1$ or $E1$	$5.7(-2)$ or $4.8(-1)$
	234.48±0.26	$3(-3)$	K.	C		$[8.9(-3)<I<7.6(-2)]$
LG	252.45±0.15*	$9(-3)$	K. L's hidden.	C		$[3.0(-2)<I<2.6(-1)]$
KJ	261.23±0.14	$8(-3)$	K. L's hidden. Probably 186.	C		$[2.9(-2)<I<2.5(-1)]$
MG	268.98±0.14	$1.2(-2)$	K. L_1 hidden. Absence of L_3.	C	not $E2$ $M1$ or $E1$	$5.1(-2)$ or $4.6(-1)$
PM	272.80±0.16	$4.3(-3)$	K. L hidden.	C		$[1.9(-2)<I<1.7(-1)]$
VR	276.54±0.14*	$1.2(-3)$	K, L_1. Absence L_3. $K/L_1=12\pm5$.	B	$M1$ or $E1$	$4.7(-3)$ or $4.8(-2)$
NG	284.26±0.15*	$5(-3)$	K, L_2. L_3, M hidden. $K/L_2=4\pm2$.	B	prob $E2$	$8(-2)$
PL	288.80±0.12*	$1.3(-2)$	K, L_1 or $L_{1,2}$. L_3, M hidden.	B		$[4.7(-2)<I<4.8(-1)]$
	292.98±0.20	$5(-3)$	K. L hidden. Possibly 187.	C		$[2.4(-2)<I<2.5(-1)]$
CB	296.75±0.06*	$9.95(-1)$	K, $L_{1,2}$, L_3, M. $K/L_{1,2}/L_3/M=(1.00\pm0.04)/(0.27\pm0.01)/(0.100\pm0.005)/(0.095\pm0.005)$.	A	$E2$	1.8(+1)
KE	299.45±0.29	weak		C		
HF	302.86±0.11*	$8(-3)$	K. L's, M hidden. Decay scheme.	B	($E2$)	$1.6(-1)$
	305.59±0.11	$7(-3)$	K. L's, M hidden.	C		$[4.0(-2)<I<3.7(-1)]$
	309.64±0.12	$1.6(-2)$	K, M. L's hidden. $K/M=18\pm7$.	B		$[9.4(-2)<I<8.9(-1)]$
JM	311.85±0.15	$8(-3)$	K. L's hidden.	C		$[4.7(-2)<I<4.4(-1)]$
	321.16±0.19	$3(-3)$	K, L_2. $K/L_2=1.4\pm1$.	B	$E2$	$5.8(-2)$
	322.63±0.17	$5(-3)$	K. L hidden.	C		$[2.9(-2)<I<2.7(-1)]$
	326.55±0.21	$3(-3)$	K. L hidden. Possibly 187.	C		$[1.8(-2)<I<1.7(-1)]$
	330.22±0.17	$3(-3)$	K, $L_{1,2}$. L_3, M hidden. $K/L_{1,2}=2.5\pm1.8$.	B	$E2$	$7.7(-2)$
FC	334.02±0.17	$5(-3)$	K, $L_{1,2}$. L_3, M hidden. $K/L_{1,2}=1.8\pm0.8$.	B	$E2$	$1.3(-1)$
	342.50±0.12	$5(-3)$	K. L's hidden.	B		$[3.8(-2)<I<3.6(-1)]$
	351.73±0.13	$1.7(-2)$	K, $L_{1,2}$. L_3, M hidden. $K/L_{1,2}=3.7\pm1.4$.	A	$E2$	$4.6(-1)$
IG	364.90±0.18*	$5(-3)$	K. L's hidden.	C		$[4.7(-2)<I<4.3(-1)]$
	387.93±0.18	$4(-3)$	K. L's hidden.	C		$[3.8(-2)<I<3.5(-1)]$
	403.29±0.16	$4(-3)$	K. L's hidden.	C		$[3.7(-2)<I<3.4(-1)]$
ID	406.55±0.18*	$2(-3)$	K. L's hidden.	C		$[2.4(-2)<I<2.2(-1)]$
MF	411.73±0.53	$3(-3)$	K. L's hidden.	C		$[3(-2)<I<2.8(-1)]$

* See discussion of gamma-ray spectra in text.

TABLE V (*continued*).

(1) Designation	(2) E_γ (keV)	(3) Conversion line intensity	(4) Conversion lines observed, basis of multipole assignment, remarks	(5) Class	(6) Multipole assignment; transition intensity (25≅100% of Ir^{186} transitions)	
JH	420.74±0.14*	1.8(−2)	K, $L_{1,2}$. L_3, M hidden. Decay scheme.	B	($E2$)	7.5(−1)
NF	426.34±0.33*	4(−3)	K. L hidden. Possibly 185.	C	[4.7(−2)<I<4.3(−1)]	
DC	434.78±0.08*	1.89(−1)	K, $L_{1,2}$, L_3, M, N. $K/L_{1,2}/L_3/M/N=(1.9\pm0.04)/(0.45\pm0.02)/(0.11\pm0.04)/(0.14\pm0.01)/(0.05\pm0.01)$.	A	$E2$	8.5(0)
	441.50±0.17	1.1(−2)	K, L_1. $K/L_1=6\pm4$.	B	$M1$ or $E1$	2.7(−1) or 2.5(0)
	451.36±0.64	weak	K.	C		
	456.86±0.65	weak	K.	C		
	467.81±0.28	2.7(−3)	K. L's hidden.	C	[4.1(−2)<I<3.8(−1)]	
KI GC	476.90±0.21*	3.8(−3)	K, $L_{1,2}$. L_3 hidden. $K/L_{1,2}=1.9\pm0.7$.	B	$E2$	2.5(−1)
	515.50±0.26	2.4(−3)	K.	C	[4.9(−2)<I<4.2(−1)]	
	525.65±0.38	1(−3)	K.	C	[2.0(−2)<I<1.7(−1)]	
PG	542.17±0.38*	1.5(−3)	K.	C	[3.1(−2)<I<2.6(−1)]	
QG	551.43±0.30*	1.4(−3)	K. Complex line.	C	[2.9(−2)<I<2.4(−1)]	
	557.99±0.42	1(−3)	K.	C	[2.2(−2)<I<2.0(−1)]	
TJ	565.42±0.36*	3(−3)	K. L's hidden.	C	[6.3(−2)<I<5.8(−1)]	
SQ	570.31±0.49	6(−4)	K.	C	[1.4(−2)<I<1.3(−1)]	
ED	584.42±0.19	1.6(−2)	K, $L_{1,2}$, M. $K/L_{1,2}/M=(1.6\pm0.08)/(0.41\pm0.06)/(0.16\pm0.05)$. $(e^-_{584}+e^-_{622}+e^-_{630}+e^-_{636})/\Sigma\gamma_{584,622,630,636}$ is consistent[a] of $E2$ to each of the γ's.	A	$E2$	1.3(0)
QD	592.40±0.91*	8.0(−4)	K.	C	[2.1(−2)<I<1.8(−1)]	
RI	599.58±0.69*	9.3(−4)	K.	C	[2.3(−2)<I<2.0(−1)]	
JD	622.15±0.21*	8.9(−3)	K. L under K684.81. $K/L_{1,2}=\sim4$. $E2$ from level scheme. (See note under 584.)	B	($E2$)	8.6(−1)
FB	630.31±0.21*	1.2(−2)	K, $L_{1,2}$. $K/L_{1,2}=4\pm1$. (See note under 584.)	A	$E2$	1.2(0)
HC	636.23±0.21*	1.8(−2)	K, $L_{1,2}$. $K/L_{1,2}=5\pm1$. (See note under 584.)	A	$E2$	1.8(0)
	649.78±0.70	2.8(−3)	K.	C	[9.8(−2)<I<7.5(−1)]	
VJ	661.86±0.71*	1.7(−3)	K, $L_{1,2}$. $K/L_{1,2}=4\pm4$.	C	[6.0(−2)<I<5(−1)]	
RN	679.49±0.49*	1.2(−3)	K.	C	[4(−2)<I<3(−1)]	
PF	684.81±0.41*	2.2(−3)	K. L?	C	[9(−2)<I<7(−1)]	
QF	693.65±0.41*	2(−3)	K.	C	[8(−2)<I<7(−1)]	
	705.72±0.94	1.8(−3)	K.	C	[7(−2)<I<6(−1)]	
RL	712.65±0.41*	2.4(−3)	K.	C	[1(−1)<I<8(−1)]	
LC	729.48±0.42*	2.7(−3)	K.	C	[1(−1)<I<8(−1)]	
MC	745.1 ±1.4	9.2(−4)	K.	C	[5(−2)<I<3(−1)]	
NC	760.03±0.40*	1.2(−3)	K.	C	[6(−2)<I<4(−1)]	
FA	767.30±0.25*	1.0(−2)	K, $L_{1,2}$. $K/L_{1,2}=4.0\pm0.8$. $(e^-_{767}+e^-_{773})/\Sigma\gamma_{767,773}$ is consistent[a] with assignment of $E2$ to each γ.	A	$E2$	1.5(0)
GB	773.06±0.26*	1.6(−2)	K, $L_{1,2}$. $K/L_{1,2}=5\pm1$. (See note under 767.)	A	$E2$	2.4(0)
TI	780.83±0.42*	2.1(−3)	K.	C	[1(−1)<I<8(−1)]	
	794.2 ±1.2	6(−4)	K.	C	[4(−2)<I<3(−1)]	
RH UI	805.47±0.51*	2.7(−3)	K, $L_{1,2}$. $K/L_{1,2}=4\pm2$.	B	[1(−1)<I<1(0)]	
IC	841.31±0.30*	7.2(−3)	K, $L_{1,2}$. $E2$ from decay scheme. $K/L_{1,2}=5\pm2$.	A	$E2$	1.3(0)
KD	884.97±0.98	5(−4)	K.	C	[4(−2)<I<3(−1)]	
HB	933.18±0.33*	5.9(−3)	K, $L_{1,2}$, M. $E2$ from decay scheme. $K/L_{1,2}/M=(6\pm1)/(1.4\pm0.3)/(1.1\pm0.3)$. $(e^-_{933}+e^-_{943})/\Sigma\gamma_{933,943}$ is consistent[a] with assignment of $E2$ to 933γ and perhaps $M1$ to 943.	A	$E2$	1.2(0)
	943.56±0.40	3.6(−3)	K. (See note under 933.)	B	$M1$?	3(−1)
WI	959.6 ±1.5*	4(−4)	K.	C	[3(−2)<I<2(−1)]	
UH	1011.08±0.50*	1.7(−3)	K, $L_{1,2}$. $K/L_{1,2}=\sim4$.	C	[2(−1)<I<1(0)]	

TABLE V (*continued*).

(1) Designation	(2) E_γ (keV)	(3) Conversion line intensity	(4) Conversion lines observed, basis of multipole assignment, remarks	(5) Class	(6) Multipole assignment; transition intensity (25≅100% of Ir^{186} transitions)
PC	1017.9 ±2.0*	2(−4)	K. Possibly Ir^{185}.	C	[2(−2)<I<1(−1)]
LB, QC	1026.54±0.32*	3.8(−3)	K, $L_{1,2}$. $K/L_{1,2}$=∼7. See 1057.08.	B	($M1$) 4(−1)
JC, NB	1057.08±0.37*	2.9(−3)	K, $L_{1,2}$, M. $E2$ from level scheme. $K/L_{1,2}/M$=(0.3±0.1)/(0.08±0.02)/(0.04±0.02). $(e^-_{1057}+e^-_{1026})/\Sigma\gamma_{1057,1026}$ indicates[a] 1026 is $M1$ if 1057 is $E2$.	B	($E2$) 7.6(−1)
RF	1107.1 ±1.5*	8(−4)	K.	C	[1(−1)<I<7(−1)]
	1138.8 ±2.0	2(−4)	K. Possibly 185.	C	[4(−2)<I<2(−1)]
	1148.1 ±2.0	2(−4)	K. Possibly 185.	C	[2(−2)<I<1(−1)]
UG	1171.53±0.52*	1.6(−3)	K.	C	[2(−1)<I<1(0)]
TD	1187.90±0.36*	2.0(−3)	K, $L_{1,2}$. $K/L_{1,2}$=6±4.	B	[3(−1)<I<2(0)]
SF	1264.65±0.80*	6(−4)	K. Possibly 185.	C	[1(−1)<I<6(−1)]
PB, UF	1314.36±0.59*	1.0(−3)	K, $L_{1,2}$. $K/L_{1,2}$=3±2.	C	[2(−1)<I<8(−1)]
QB, WG	1323.69±0.65*	7(−4)	K.	C	[1(−1)<I<7(−1)]
RC	1439.9 ±1.5*	6(−4)	K.	C	[1(−1)<I<6(−1)]
WF	1467.1 ±1.8	3(−4)	K.	C	[8(−2)<I<3(−1)]
	1508.05±0.72	1.2(−3)	K.	B	[4(−1)<I<2(0)]
SC	1597.14±0.84*	7(−4)	K.	C	[3(−1)<I<1(0)]
TC	1621.7 ±2.0*	3(−4)	K. Possibly 185.	C	[1(−1)<I<4(−1)]
UC	1647.42±0.63*	2.0(−3)	K, $L_{1,2}$. $K/L_{1,2}$=∼4.	A	[7(−1)<I<3(0)]
	1700.99±0.74	1.2(−3)	K, $L_{1,2}$. $K/L_{1,2}$=∼3.	B	[5(−1)<I<2(0)]
RB	1737.8 ±2.0*	4(−4)	K. Possibly 185.	C	[1(−1)<I<5(−1)]
	1751.36±0.86	6(−4)	K, $L_{1,2}$. Possibly 185. $K/L_{1,2}$=∼3.	B	[2(−1)<I<9(−1)]
	1789.0 ±2.0	4(−4)	K. Possibly 185.	C	[1(−1)<I<6(−1)]
WC	1800.1 ±2.5	4(−4)	K. Possibly 185.	C	[1(−1)<I<6(−1)]

used in support; results of those measurements are given below.

B. POSITRON, GAMMA-RAY, AND COINCIDENCE MEASUREMENTS

1. Positron Spectrum

The positron spectrum, measured earlier with an intermediate image spectrometer, was remeasured with one of the two thick lenses which make up the Gerholm coincidence spectrometer.[31] For this measurement the transmission was set at 3%; a special baffle was used to stop negatively charged particles. Source thickness and instrumental resolution were such as to produce a line breadth of 3.5% for the K conversion line of the 297-keV transition. A Fermi plot is shown in Fig. 4. The positron spectrum has been resolved into components having end-point energies of 1.94±0.02 MeV and 1.37±0.05 MeV and intensities relative to K 297 of 0.46±0.12 and 0.12±0.03, respectively. There may be present a weak component with an end-point energy ∼1.0 MeV. Since K 297 represents 4.1% of the Ir^{186} decays, the positron intensity is (2.5±0.7)%. Corroborative information about the positron decay was obtained from coincidence results to be presented below.

2. Gamma-Ray Measurements

Gamma-ray "singles" spectra were measured with a 3 in.×3 in. cylindrical NaI scintillation detector and a 256-channel pulse-height analyzer. Lead absorbers were used when it was desirable to attenuate intense low energy radiations. The energy range extended from 0.13 to 3.0 MeV. Most of the gamma rays known to exist from the conversion data were incompletely resolved in the scintillation spectrum. It was possible, however, to derive some quantitative information from these gamma-ray data. For example, the relative intensities of the transitions producing the 137-, 297-, and 434-keV gamma-ray peaks were calculated[32,33] to be

[31] T. R. Gerholm, Rev. Sci. Instr. **26**, 1069 (1955). We are indebted to Dr. Gerholm, Dr. J. Lindskog, and others of the Institute of Physics, Uppsala, Sweden, for the design, construction, and testing of the spectrometer, and wish to express our appreciation.

[32] The photopeak efficiency data used were those of N. H. Lazar, R. C. Davis, and P. R. Bell, Nucleonics **14**, No. 4, 52 (1956).

[33] Conversion coefficients were taken from M. E. Rose, *Internal Conversion Coefficients* (North-Holland Publishing Company, Amsterdam, 1958).

1.00:0.80:0.41. The gamma-ray intensity data were normalized relative to the internal conversion-line intensities by the adoption of the theoretical $E2$ conversion coefficient for the 434-keV transition. Internal conversion coefficients could thus be computed for a number of gamma-ray lines and from these their multipole orders were deduced. These results are included in Table V. Corrections were made for transmission through absorbers and for relative photopeak scintillator efficiencies.

Gamma rays of energy above 1.6 MeV, which were detected with the 3 in.×3 in. scintillator, were measured at higher resolution with a three-crystal pair spectrometer. The center crystal of this instrument was a $1\frac{1}{2}$ in. ×3 in. cylinder of NaI; the side crystals were 3 in.×3 in. NaI cylinders. Energies and relative intensities of the gamma rays observed are given in Table VI.

TABLE VI. Three-crystal pair spectrometer measurements of the high-energy gamma rays of Ir^{186}.

Energy (MeV)	Relative intensity
1.60 to 1.75	1.0 (complex)
2.34±0.03	0.14±0.03
2.53±0.04	0.08±0.02
2.76±0.05	0.20±0.04
2.89±0.05	0.04±0.01

3. Coincidence Measurements

In the sources used for the coincidence measurements, the radiations of Ir^{185} and Ir^{187} were weaker in intensity than those of Ir^{186} by approximately a factor of ten. Possible contributions from these contaminants to the various coincidence counting rates have been estimated and are, in almost all cases, negligible.

a. Three types of measurements were made with the Gerholm electron-electron coincidence spectrometer.

(i) With one magnetic lens set for positrons of (1.50±0.06)-MeV energy and with a cylindrical 1 in. ×$1\frac{1}{2}$ in. NaI gamma-ray detector, coincidences were observed of positrons with x rays and with gamma rays of energies 137, 297, and 434 keV. The coincidence resolving time used was $2\tau=0.18$ μsec. After correction for conversion and detector efficiency, the transition intensities corresponding to the three gamma rays were found to be equal within 15%. This result shows that the positron transition of highest energy populates the state at 868 keV.[5]

(ii) Replacement of the scintillation detector by the second magnetic lens made possible the measurement of positron-conversion-electron coincidences. With one lens set as before for the positrons, conversion electrons of the 137-, 297-, and 434-keV transitions were observed in coincidence. The relative transition intensities as computed from these results were again equal within statistical errors of about 30%.

(iii) Electron-electron coincidences also were investigated with the two lens arrangement. With one lens set for L 137, coincidences were observed with peaks due to K conversion of the following transitions: 297 keV; 434 keV; 622, 630, and 636 keV (unresolved); 767 and 773 keV (unresolved); and 933 and 943 keV (unresolved). Comparison of the coincidence intensities with intensities in "singles" conversion spectra shows that the 137-keV transition is coincident with each of the 622-, 630-, and 636-keV transitions; that it is coincident with one but not both of the 767- and 773-keV transitions; and that it is coincident with one or both of the 933- and 943-keV transitions.

b. Measurements of gamma-ray–gamma-ray coincidences were made with a pair of cylindrical NaI scintillation detectors, one 2 in.×3 in. and one 3 in.×3 in. A coincidence circuit with resolving time $2\tau=1.4\times10^{-7}$ sec was used to gate a pulse-height analyzer,[34] which recorded in each of 32 amplitude channels for the 2 in.×3 in. detector a 64-channel spectrum of pulses occurring in coincidence in the 3 in.×3 in. detector. The two detectors were shielded from each other by lead gamma-ray absorbers. Two sets of measurements were made to span different energy ranges in the 64 channels. In one case the range was 600 keV to 3 MeV; lead absorbers, ~2 g/cm², served to shield both detectors from low-energy photons. In the second case, the range was 200 to 1200 keV, and the lead absorber was removed from the 3 in.×3 in. detector. The energy range for the 2 in.×3 in. detector was from 150 to 900 keV. In each case the spectrum of accidental coincidences was constructed from the observed "singles" spectra of the two detectors by assembly into a two-dimensional pulse-amplitude matrix of the channel by channel products of the singles spectra; these products were normalized so that the total rate of accidental coincidences derived from the constructed spectrum equalled the rate of accidental coincidences observed on a scaler when a delay was inserted between one detector and the coincidence circuit.

In the net true spectrum several peaks were observed representing gamma-gamma coincidence events with full energy absorption of both gamma rays in the scintillators; with corrections for efficiency of the detector,[32] their abundances could be determined relative to 434–297-keV coincidences. Results of these comparisons will be given in the discussion of individual levels in Os^{186}.

From annihilation-434-keV and annihilation-297-keV coincidences it was possible to compute a value (3±1)% for the fraction of Ir^{186} decay which proceeds by positron emission. This value, to which a relatively large uncertainty is attached because of the difference between annihilation source volume and gamma-ray source volume, is in agreement with the positron intensities measured by magnetic spectrometry, as described earlier.

[34] R. L. Chase, Proc. Inst. Radio Engrs. 47, 464 (1959).

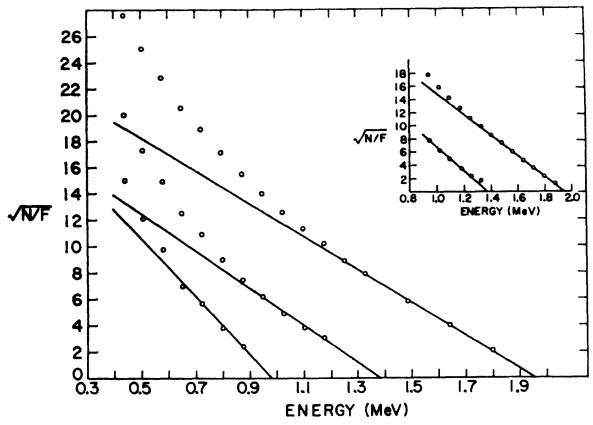

FIG. 4. Fermi analysis of the positron spectrum of Ir^{186}. Data, shown in the inset, which were obtained in an independent set of measurements at the upper energy end, were used to establish the two higher energy components.

III.

A. CONSTRUCTION OF THE LEVEL SCHEME

The level scheme was constructed in the following way: With the aid of an electronic computer, energy sums were formed for all possible twofold combinations of the 101 transitions listed in Table V. These energy sums were arranged in a matrix and also in a list in order of increasing energy. Cascade-crossover relationships of the type $E(\gamma_1)+E(\gamma_2)=E(\gamma_3)$ were then investigated. Possible levels established were examined for additional connections to other levels. The search was first restricted to energy sums involving the previously established levels: levels B (137.15 keV), C (433.91 keV), D (868.70 keV), and F (767.38 keV).[35] In this way levels G (910.33 keV) and H (1070.25 keV) were found. The search was then extended to include transitions associated with levels G and H. This resulted in the

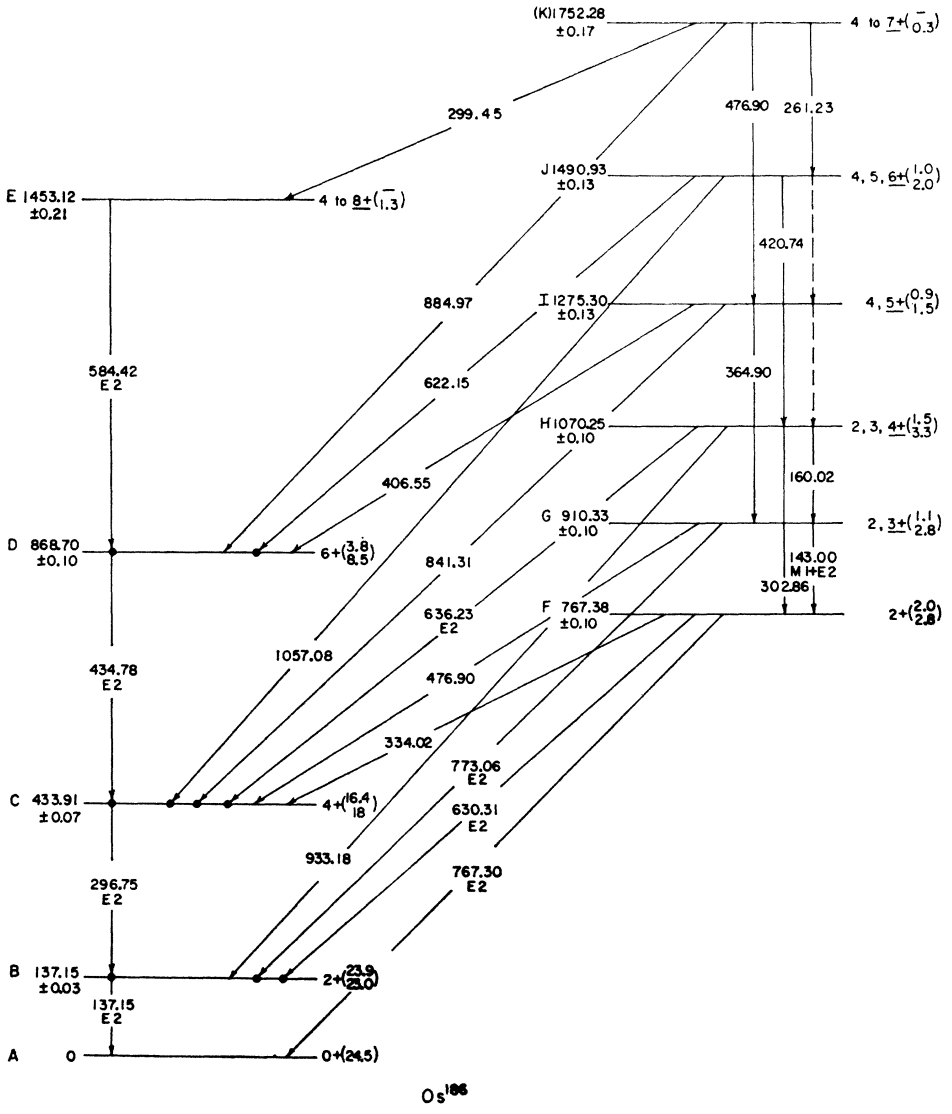

FIG. 5. A partial level scheme of Os^{186} showing those levels believed to be members of the ground-state rotational band and of the gamma-vibrational ($K=2$) band, and the transitions between them. Transitions expected to occur which could not be observed because of interfering radiations are indicated by broken lines. Energies (in keV) of transitions and their multipole orders (where established) are shown. Observed coincidences of transitions are indicated by a solid circle at the terminus of the upper transition. When the assignment of the spin and parity of a level is not uniquely determined, the most probable spin and parity are underlined. For each level the approximate incoming and outgoing intensities are given in parentheses. Intensities are taken from Table V, column 6.

[35] For convenience, the energy levels have been designated by the letters A to X. Transitions are designated accordingly, e.g. transition BA is the 137.15-keV transition.

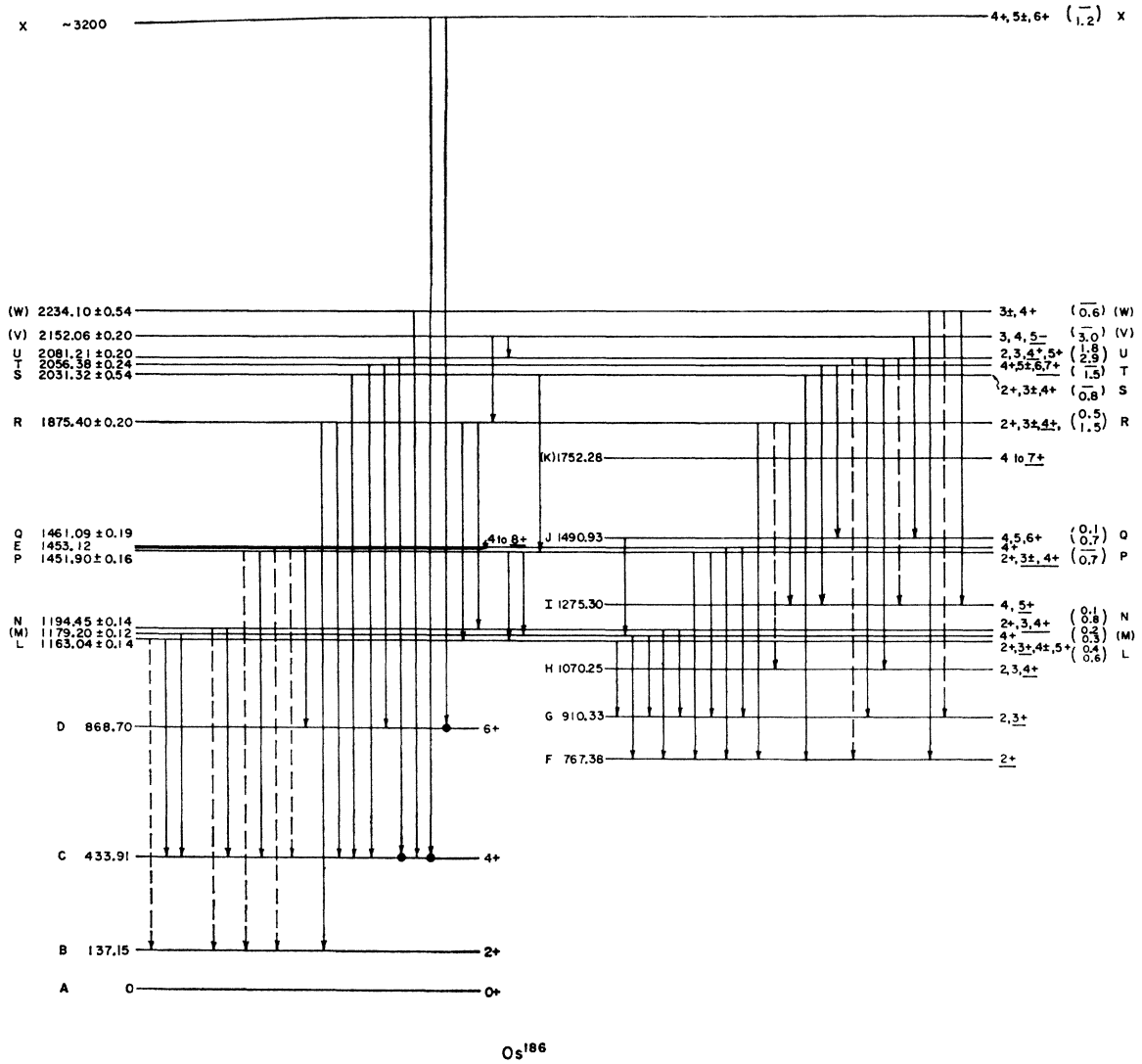

FIG. 6. Level scheme of Os^{186} including all of the energy levels presently established. Only those transitions are shown which are not included in the partial level scheme of Fig. 5. Transitions which fit in more than one location in the level scheme are indicated by dotted lines. Other information shown is indicated in the same way as in the preceding figure.

placing of several additional levels, including levels I through W, shown in Figs. 5 and 6.

Because of the large number of chance energy sum relationships, it is necessary to estimate the probability that a level, although apparently connected by a number of transitions to other levels, may actually be false. Such an estimate is made in Appendix II, in which it is shown that on statistical considerations alone ~4 spurious levels may be expected. Therefore, each level found in this way was considered in the light of additional available evidence, such as (1) coincidence data, (2) the flow of intensity in and out of the level, (3) consistency of transitions with plausible selection rules, and (4) the pattern of transitions in and out of levels believed to have collective character.

On these grounds a number of possible levels have been omitted from the final scheme. Consequently, it is estimated that no more than 1 or 2 of the levels finally included may be spurious.

The energies of the levels have been calculated with the use of the method of least squares. Only the energies of the better established transitions were used in this calculation; these transitions are designated by an asterisk (*) in Table V.

B. PROPERTIES OF THE LEVELS

In the following paragraphs properties of the individual levels are discussed. An attempt is made to draw a clear distinction between those properties which follow as a logical consequence of the present results and those which appear probable from the present results or from the systematics of the properties of nuclear energy levels.

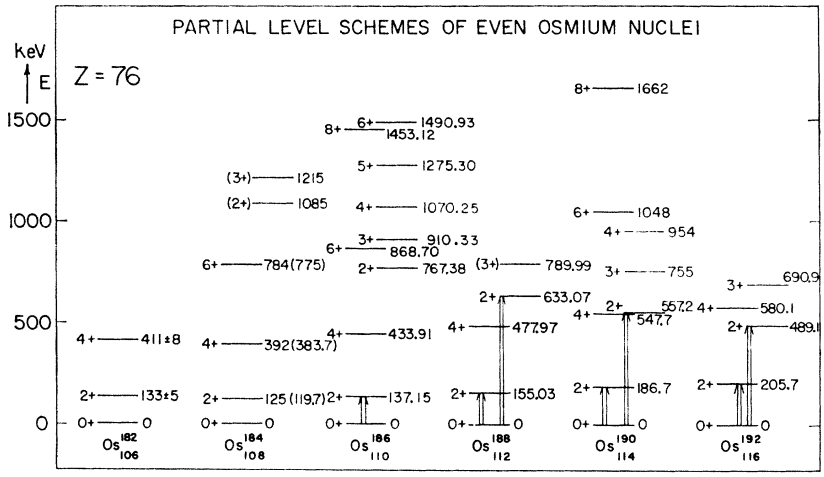

FIG. 7. Partial level schemes of even-A osmium nuclei. Only levels deemed to belong to the ground-state rotational band (at left) and to the gamma-vibrational band (at right) are given for each isotope. If a level has been reached by Coulomb excitation, this is indicated in the usual manner.[††] The spins and energy values are taken from the following references. Os^{182} and Os^{184}: R. M. Diamond, J. M. Hollander, D. J. Horen, and R. A. Naumann, Nucl. Phys. **25**, 248 (1961); energy values without parentheses. Os^{184}: V. I. Baranov, K. Ya. Gromov, B. S. Dzhelepov, Zyong Chang Bai, T. V. Malysheva, V. A. Morozov, B. A. Khotin, and V. G. Chumin, Izvest. Akad. Nauk (SSSR) Ser. Fiz. **24**, 1079 (1960) [translation: Bull. Acad. Sci. U.S.S.R. **24**, 1066 (1960)]; energy values in parentheses. Os^{186}: present work. Os^{188}: Graham, Geiger, Naumann, and Prospero, reference 29, and references cited there. Os^{190}: Kane, Emery, Scharff-Goldhaber, and McKeown, reference 2, and references cited there. Os^{192}: The values for the energies of the transitions stem from L. L. Baggerly, P. Marmier, F. Boehm, and J. W. M. Du Mond, Phys. Rev. **100**, 1364 (1955); the location of the second 2+ state is derived from Coulomb excitation work (references 45, 46). Spins and energies of the higher levels, which have been deduced from the systematics of level schemes in this region, are compatible with all existing information.

For clarity, the level scheme has been divided into two parts. In the first part, in Fig. 5, only those levels are included which are believed to be members of the ground-state rotational band or the $K=2$ band, and the transitions between them are shown. In the second part, in Fig. 6, all remaining levels are added and only the transitions from the added levels are shown. Coincidences of gamma rays are indicated in the level scheme. For each level, the spins and parities consistent with the present results are given, and the most probable spin and parity are underlined. For this purpose, where the multipole orders of transitions are not definitely established, it is assumed that all transitions are of $E1$, $E2$, or $M1$ multipole order. The estimated total transition intensities into and out of each level are also shown.[36]

Levels B (137.15 keV), C (433.91 keV), and D (868.70 keV)

The properties of these levels as members of the ground-state rotational band were established in previous work, so that the present results add little new information concerning them.

The total intensities of transitions in and out of level B are seen to be almost equal; the same is true for level C. For level D, however, there is a large excess of transition intensity out over the transition intensity in. This is consistent with gamma-positron coincidence results obtained in the present work indicating that level D is the lowest level populated directly by the decay of Ir^{186}.

Level E (1453.12 keV)

The existence of this level is supported by two transitions; a strong $E2$ transition to level D and a weak transition from level K, which may be the 7+ member of the gamma band. Additional support is given by the observation that transition ED is coincident with transitions DC and CB and not coincident with the group of transitions JD–FB–HC (which appear as one peak in a sodium iodide gamma spectrum), all of which originate in the gamma band. The $E2$ character of transition ED restricts level E to even parity and a spin of 4 to 8. The nonappearance of transitions EC, EB, or EA suggests that the spin of level E is 7 or 8. Finally the end-point energy, 1.37±0.05 MeV, and the intensity of the second positron group indicate that level E and probably also level J are populated by this group (cf. Sec. IIIC). From this evidence and from its energy, which fits into the trend of the level energies of the even osmium nuclei (cf. Figs. 7, 8), level E is tentatively assigned as the 8+ member of the ground-state rotational band.

Level F (767.38 keV)

In previous work level F was shown to be the second 2+ state of Os^{186}. From its 2+ character and its energy, it is presumably the lowest level of the $K=2$ (gamma-vibrational) band.

[36] For those transitions whose multipole orders could not be established, intensities were estimated to be the geometric mean of those calculated from $E1$ and $M1$ conversion coefficients. This estimate corresponds approximately to the value for $E2$ multipole order.

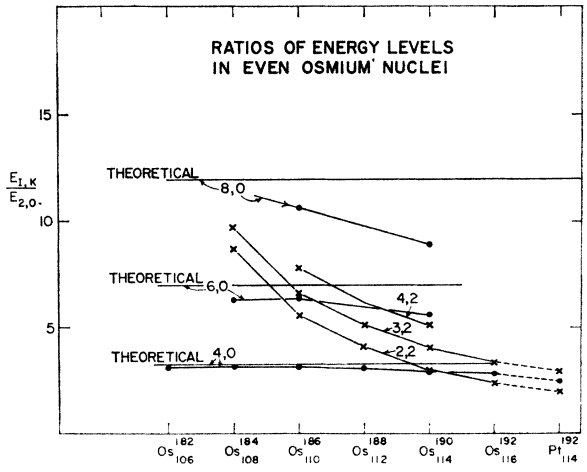

FIG. 8. Ratios $E(IK)/E(20)$ are plotted for even-A osmium isotopes. The horizontal lines indicate the ratios for the ground-state band in the strong-coupling limit, where $E \sim I(I+1)$. It is seen that: (a) The ratios for the ground-state band decrease gradually as N increases. (b) The 2+ state of the gamma-vibrational band decreases rapidly as N increases and finally moves below the 4+ state of the ground-state band (in Os^{192}). (c) The spacing between the 2+ and 3+ states of the gamma-vibrational band indicates that the moments of inertia of the two bands differ only by 1–6%. The spacing between the 3+ and 4+ states of the gamma band, on the other hand, is somewhat smaller than would correspond to the same moment of inertia, especially in the case of Os^{190}, where the 4+ state is probably depressed by a higher lying 4+ state. The corresponding ratios for Pt^{192} are also shown. The same level order as in Os^{192} exists in this isotope, but the ratios are all somewhat lower.

Level G (910.33 keV)

From the $E2$ character of transition GB, the existence of transition GC, and the fact that the K/L ratio of transition GF indicates mixed $M1-E2$ character,[37] level G is assigned even parity and a spin of 2 or 3. The absence of a ground-state transition GA suggests that level G is 3+. From this evidence and its energy, level G is identified as the 3+ member of the $K=2$ band.

Level H (1070.25 keV)

From the existence of transitions HG, HF, HC, and HB, and a lower limit on the internal conversion coefficient of transition HB, which rules out $E1$ multipole order, level H must have even parity and a spin of 2, 3, or 4. The absence of a ground-state transition HA suggests that the spin is 3 or 4. From this evidence and the energy of level H, it is tentatively identified as the 4+ level of the $K=2$ band.[38]

Level I (1275.30 keV)

From the existence of transitions IG, IC, and ID, and a lower limit on the internal conversion coefficient of transition IC, which rules out $E1$ multipole order, level I must have even parity and a spin of 4 or 5. Transition IH (205.05 keV), which would be expected to appear, was not observed; this may be due to the fact that the position of its K internal conversion line was obscured by a line of another, stronger transition. The absence of a transition IF suggests that the spin is 5. From this evidence, and the energy of level I, it is tentatively identified as the 5+ level of the gamma band. In possible contradiction to this assignment, there exists an 1138.8-keV transition which has the correct energy to be transition IB, in which case a spin of 4 would have to be assigned to level I. It is considered more probable that the 1138.8-keV transition has its origin elsewhere in the level scheme (or possibly in the level scheme of Os^{185}) and that level I is indeed the 5+ member of the $K=2$ band.

Level J (1490.93 keV)

From the existence of transitions JH, JD, and JC, and a lower limit on the internal conversion coefficient of transition JD, which rules out $E1$ multipole order, level J must have even parity and a spin of 4, 5, or 6. Transition JI (215.64 keV), which would be expected to appear, was not observed, possibly because the position of its K internal conversion line was obscured by a line of another, stronger transition. The absence of transitions JG, JF, and JB suggests that the spin is 6. As is shown in Sec. IIIC, this level appears to be populated directly by positron emission. From this evidence, and the energy of level J, it is tentatively identified as the 6+ member of the $K=2$ band.

Level L through X

The remaining levels are shown in the level scheme of Fig. 6. All, save for level X, were established from internal conversion data supported in some instances by gamma-gamma coincidence results. Level X was established from gamma-ray singles spectra obtained with a three-crystal pair spectrometer and from gamma-gamma coincidence results. The spins and parities assigned to the levels follow directly from the properties of the transitions listed in Table V.

Most of these levels appear to decay to members both of the ground-state band and of the $K=2$ band, as well as to one another. Because only those levels which are connected by a number of transitions to other levels

[37] The total intensity and K/L ratio of transition GF are suspect, however, in that they both appear inordinately large; i.e., the relative reduced transition probability of transition GF and its apparent large $M1$ admixture are not in accord with theoretical expectations. In the internal conversion spectrum the line breadth and density of lines in the vicinity of the K internal conversion line of transition GF are such that the probability that any peak is actually an unresolved doublet of lines is ≈ 0.1. Thus the peaks identified as the K and L_{II} internal conversion lines of transition GF may actually have second components, and hence the properties of transition GF should be regarded as only tentatively established.

[38] The apparent total intensity of transition HG, like that of GF, is unexpectedly large; its properties must be regarded as only tentatively established.

could be established with a high degree of confidence, there undoubtedly exist a number of other, as yet unidentified, levels in this energy region. Additional data will be necessary before this part of the level scheme can be elucidated and the collective or individual particle nature of these levels established.

C. POSITRON DECAY AND THE GROUND STATE OF Ir^{186}

The fact that the most energetic positron group, 1.94 MeV, populates level D, which has been assigned a spin of 6, considered together with the value 7.9 for $\log ft$ of this transition, suggests for the ground state of Ir^{186} odd parity and spin 6 or 7, although even parity cannot be excluded. Furthermore, with the assumption that the intensity not accounted for in the population of level D [(electromagnetic transition intensity)$_{out}$ − (electromagnetic transition intensity+positron intensity)$_{in}$] is the electron-capture intensity from Ir^{186}, the K/β^+ ratio for this beta transition is calculated to be 6.5 ± 3, a value consistent with the value 5.7 expected[39] for either an allowed transition or a once forbidden transition with spin change 0 or 1. The energy of the inner group, 1.37 MeV, is the value expected for direct population of levels E, spin 8, or J, spin 6; and there appears to be little or no direct population of level I, spin 5. The $\log ft$ value for this positron group is 7.8, or, if it has two equal intensity components for E and J, each would have $\log ft \approx 8.1$. In the manner described above, the K/β^+ ratio for the transition to level E, with the assumption of two branches, would be 17; this is just the theoretical value for an allowed transition or approximately that for a nonunique first-forbidden one. These facts weigh against an assignment of spin 6 to Ir^{186} and are consistent with spin 7 for this nuclide. Thus the lowest energy positron component, of approximately 1.0 MeV end-point energy, possibly populates level K.

IV.

A. OSMIUM 186 AND OTHER EVEN-MASS OSMIUM NUCLEI

The level scheme of Os^{186} will now be discussed in the framework of our knowledge of the spectra of the even-mass Os isotopes.

Since it was first pointed out[1] that the even osmium nuclei present the only region in the periodic system in which a *gradual* transition from the strongly deformed to the near-harmonic level pattern may be observed—in contrast to the two other transition regions, that between 88 and 90 neutrons[40,41] and that between 86 and 88 protons,[42] which are more abrupt—a great deal of new information has been accumulated.

In Fig. 7 the present information on the ground-state ($K=0$) band and the $K=2$ (gamma-vibrational) band of each of the even-mass Os nuclei is summarized. Although many additional levels are known for the nuclei Os^{186}, Os^{188}, and Os^{190}, they are not included in this figure to avoid confusion. The most striking features emerging from this summary are (1) the gradual increase of the energies of the levels of the ground-state band, and (2) the decrease of the energies of the levels of the $K=2$ band, as the neutron number increases. In Fig. 8, the same information is presented, but this time the ratios E_{IK}/E_{20} are shown. Here E_{IK} denotes the energy of the state with angular momentum I, whose component along the axis of symmetry is K. It is seen that the deviation of the ratios for the levels of the ground-state band from the strong coupling values (which are indicated by horizontal lines) increases slowly with increasing neutron number, whereas the ratios for the members of the $K=2$ band come down quite rapidly. For comparison, the corresponding level ratios for Pt^{192} are indicated at the right of Fig. 8. Although this nucleus has 2 fewer neutrons than Os^{192}, all the known level ratios are appreciably lower, but the same level order is preserved. It further appears that the curves for the (2,2), (3,2), and (4,2) states are fairly parallel. Closer inspection shows that the spacing between the curves (2,2) and (3,2) is approximately one, indicating that the moments of inertia of the ground-state and $K=2$ bands are approximately the same. A more quantitative comparison will be given in Sec. IV.B.

It may further be remarked that, in addition to the levels shown in Figs. 7 and 8, other levels which may be of a collective character have been found in some of the even-mass Os nuclei: thus, two states with spin 0 and even parity are known in Os^{188},[43] and a third 4+ state[44] (possibly a two-phonon state) has been found in Os^{190}, as well as four odd-parity states[2,44] some of which may be members of an octopole band. Further study is needed to establish the nature of these levels and to search for the corresponding states in other even-mass Os nuclei.

Two different research groups[45,46] have been able to excite the first and second 2+ states of Os^{188}, Os^{190}, and Os^{192} by Coulomb excitation and could thus establish $B(E2)$ values for the transitions (2,2) → (0,0), (2,2) →

[39] M. L. Perlman and M. Wolfsberg, Brookhaven National Laboratory Report BNL-485, T-110 (unpublished); M. L. Perlman, J. P. Welker, and M. Wolfsberg, Phys. Rev. **110**, 381 (1958).

[40] K. Ford, Phys. Rev. **95**, 1250 (1954).

[41] G. Scharff-Goldhaber and J. Weneser, Phys. Rev. **98**, 212 (1955).

[42] G. Scharff-Goldhaber, Phys. Rev. **103**, 837 (1956).

[43] W. J. King and M. W. Johns, Can. J. Phys. **37**, 755 (1959); R. E. Arns, R. D. Biggs, and M. L. Wiedenbeck, Nucl. Phys. **15**, 125 (1960); I. Marklund, B. van Nooijen, and Z. Grabowski, *ibid.* **15**, 533 (1960).

[44] O. B. Nielsen, N. O. Roy Poulsen, R. K. Sheline, and B. Skytte Jensen, Nucl. Phys. **10**, 475 (1959).

[45] R. Barloutaud, P. Lehmann, and A. Leveque, Compt. Rend. **245**, 523 (1957), and J. Phys. Radium **19**, 60 (1958).

[46] F. K. McGowan and P. H. Stelson, Phys. Rev. **122**, 1274 (1961); F. K. McGowan, in *Comptes Rendus du Congrès International de Physique Nucléaire; Interactions Nucléaires aux Basses Energies et Structure des Noyaux, Paris, July, 1958* (Dunod Cie., Paris, 1959), p. 233.

TABLE VII. The energies of the collective levels of Os^{186} are compared with the predictions of the various models discussed in the text. The energies are in keV. Three dots indicate that the parameters of the model have been chosen to fit that level. Square brackets indicate the percentage differences from the experimental values.

(1) Level	(2) IK	(3) Experimental energy (keV)	(4) Unperturbed Bohr-Mottelson, Sec. 1	(5) Perturbed Bohr-Mottelson, Sec. 2	(6) Unperturbed Davydov, Sec. 3	(7) Perturbed Davydov, Secs. 4, 5	(8) Mallmann, Sec. 6
B	20	137.15±0.03	...	...	...	...	...
C	40	433.91±0.07	457.2[+5.4%]	...	444.5[+2.4%]	...	...
D	60	868.70±0.10	960.0[+10.5%]	833.5[−4.1%]	896.7[+3.2%]	842.9[−3.0%]	851.4[−2.0%]
E	80	1453.12±0.21	1645.8[+13.3%]	1250.9[−13.9%]	1472.6[+1.3%]	1312.6[−9.7%]	1373.7[−5.5%]
F	22	767.38±0.10	...	...	...	...	...
G	32	910.33±0.10	904.5[−0.6%]	...	904.5[−0.6%]	885.0[−2.8%]	...
H	42	1070.25±0.10	1087.4[+1.6%]	...	1104.5[+3.2%]	1048.8[−2.0%]	1141.0[+6.6%]
I	52	1275.30±0.13	1316.0[+3.2%]	...	1316.0[+3.2%]	1217.9[−4.5%]	1345.5[+5.5%]
J	62	1490.93±0.13	1590.3[+6.7%]	1404.1[−5.8%]	1658.6[+11.2%]	1467.2[−1.6%]	1788.6[+20.0%]
(K)	72	(1752.28±0.17)	1910.3[+9.0%]	1641.5[−6.3%]	1901.5[+8.5%]	1641.5[−6.3%]	1970.0[+12.4%]

(2,0), and (2,0) → (0,0). Van Patter,[47] in a study of the validity of the asymmetric rotor model of the nucleus proposed by Davydov and co-workers,[3,4] found that the ratios of these $B(E2)$ values agree fairly well with the predictions of this model. A more extensive comparison of the energies and relative transition probabilities[2] in Os^{190} showed that both sets of values are in fair agreement with the model predictions, if one assumes for Os^{190} an asymmetry parameter $\gamma \approx 22°$. In the following a similar analysis of the energies and transition probabilities of Os^{186} on the basis of various model assumptions will be given.

B. INTERPRETATION OF LEVEL ENERGIES

In this section the energies measured for the levels of Os^{186} are compared with the predictions of various nuclear models. The discussion is limited to the two identified even-parity collective bands: the ground-state band, $K=0$, with spins 0, 2, 4, 6, and 8, and the $K=2$ band, with spins 2, 3, 4, 5, 6, and possibly 7. Table VII shows the energies assigned to these levels from the experimental data. For the purpose of these comparisons, the adjustable parameters of the models have been chosen so that certain low-lying states are exactly fitted. In Sec. B.8 an attempt to make a numerical estimate of the quality of fit of the various models by means of least squares adjustments is described.

1. Strong Coupling Model

In the unperturbed strong coupling model of Bohr and Mottelson[48] the energies of the levels in the ground-state ($K=0$) and the gamma-vibrational ($K=2$) bands are given by

$$E_{I0}=\tfrac{1}{6}E_{20}I(I+1), \tag{2}$$

$$E_{I2}=E_{22}+\tfrac{1}{6}E_{20}[I(I+1)-6]. \tag{3}$$

The values for E_{IK} are given in column 4 of Table VII; the percentage deviations from the experimental values are shown in square brackets. Figure 9 presents this information graphically.

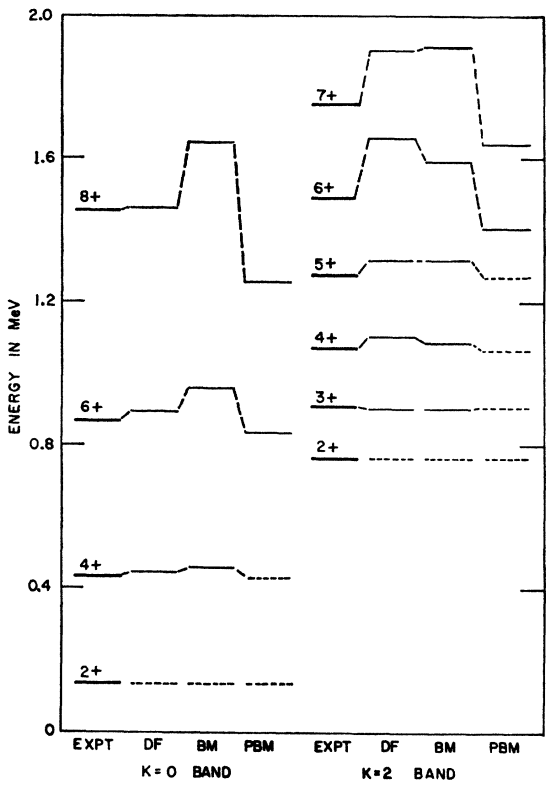

FIG. 9. A comparison of the energies predicted by some nuclear models with the experimental energies of the collective levels of Os^{186}. The parameters of each model have been chosen (as in Table VII) so that certain levels, shown by horizontal dashed lines, are fitted. DF refers to the asymmetric rotor model of Davydov and Filippov (Sec. IV. B.3), BM to the strong coupling model of Bohr and Mottelson (Sec. IV. B.1), and PBM to the strong-coupling model with rotation-vibration perturbations (Sec. IV. B.2).

[47] D. M. Van Patter, Nucl. Phys. **14**, 42 (1959).

[48] A. Bohr, Kgl. Danske Videnskab. Selskab, Mat.-Fys. Medd. **26**, No. 14 (1952); A. Bohr and B. R. Mottelson, *ibid.* **27**, No. 16 (1953); K. Alder, A. Bohr, T. Huus, B. R. Mottelson, and A. Winther, Rev. Mod. Phys. **28**, 432 (1956).

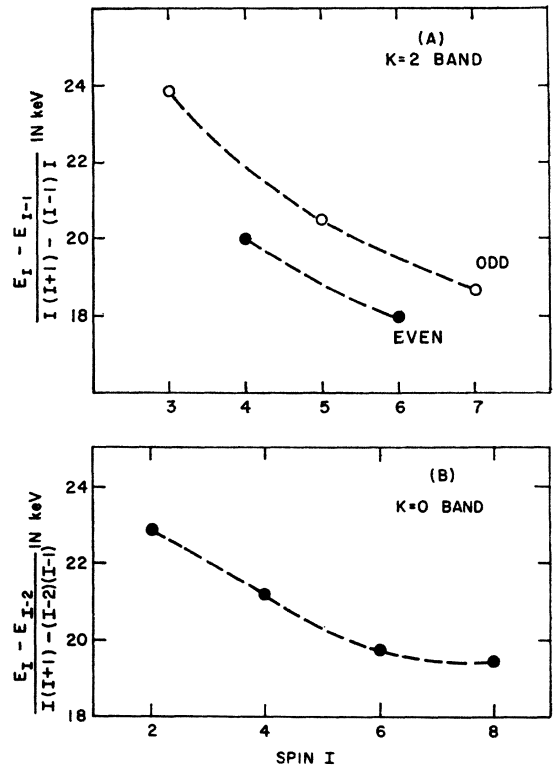

FIG. 10. (A) The experimentally observed differences in the level energies in the $K=2$ band, divided by $[I(I+1)-(I-1)I]$, are plotted against total angular momentum I. The points corresponding to even I (filled circles) are found to be shifted downward with respect to those corresponding to odd I (open circles). The spin 7 level, as noted in Sec. III, is less certain than the others. It is interesting to note that recent data on the extensive $K=2$ band in Er^{166} [C. J. Gallagher, Jr., O. B. Nielsen, O. Skilbreid, and A. W. Sunyar (unpublished); see Gallagher and Soloviev, reference 58, pp. 34–35], if plotted in the same way, do not show an odd-even shift beyond the energy uncertainties. In the Er^{166} case ($I=2$ through 7) the points lie on a single straight line whose downward slope is only about 1.2% per unit of angular momentum. (B) A similar plot is shown for energy differences in the ground-state band. For each band the simple strong-coupling model predicts that all points should lie on a horizontal line. A comparison of the experimental data with other models is given in the next figure.

Figure 10 (A) shows the energy differences between adjacent levels in the $K=2$ band, divided by the difference in the quantity $I(I+1)$ for the two levels. For a pure rotational spectrum, as given by Eq. (3), the points would lie on a straight horizontal line. It is clear from the figure that the levels of even spin are shifted downward with respect to the levels of odd spin.

The lower half of Fig. 10 shows a similar plot for the ground-state band. The deviation of all three curves in Fig. 10 from a horizontal line shows that, if the strong coupling model is to have any validity for Os^{186}, then some rotation-vibration interaction must be taken into account.

2. Strong Coupling Model with Band Mixing

With the rotation-vibration interactions included in the first nonvanishing order in perturbation theory, the energies of levels of the ground-state band may be described by

$$E_{I0}=AI(I+1)-BI^2(I+1)^2. \tag{4}$$

In the same order the predicted level energies in the $K=2$ band may indeed show an odd-even shift; the energy spacing is given by

$$E_{I2}-E_{22}=A'[I(I+1)-6]$$
$$-B'\left\{(I-1)I(I+1)(I+2)\left[\frac{1+(-1)^I}{2}\right]-24\right\}$$
$$-C'[I^2(I+1)^2-36]. \tag{5}$$

The level energies calculated from Eqs. (4) and (5) are shown in column 5 of Table VII and are also indicated in Fig. 9. The values of the constants found by fitting the lowest levels of each band are: $A=23.357$ keV, $B=0.0831$ keV, $A'=26.222$ keV, $B'=0.0378$ keV, $C'=0.1416$ keV. In the upper half of Fig. 11, the experimental data shown in Fig. 10 are compared with the predictions of Eq. (5) (solid lines). It seems that each of the last two terms of Eq. (5) is proportional to too high a power of I to fit the experimental data. A similar plot for the $K=0$ band of Os^{186} is given in the bottom half of Fig. 11. Here also, the failure of the solid curve to follow the experimental points shows that the power of I in the last term of Eq. (4) is too great, or that higher terms should be included. A term proportional to $I^4(I+1)^4$, however, is not sufficient.

3. Hydrodynamic Asymmetric Rotor Model

The results of the asymmetric rotor model proposed by Davydov and collaborators[3,4] are shown in column 6 of Table VII, and in Fig. 9. The value of γ, found by fitting the ratio of the two 2+ states, is 16.51°. The fit for the levels of the ground-state band and for the spin 3, 4, and 5 levels of the $K=2$ band is much better than for the other models, but the two highest level energies differ appreciably from the experimental values.

Though an odd-even shift in the $K=2$ band is inherent in the model, the shift is of opposite sign to that found experimentally; that is, the model predicts that the even-spin levels should be shifted upward with respect to the odd-spin levels. The comparison is shown in Fig. 11, Part A.

It should perhaps be noted that the value of γ found in a least squares fit to nine excited levels (described in Sec. B.8) is 16.4°, remarkably close to the value found from the ratio of the energies of the two lowest 2+ levels. When the strong-coupling model is fitted to the level scheme, however, there is a difference of 7% between the coefficient of $I(I+1)$ in Eq. (2) found from the experimental 20 energy and that found from the least-squares fit. A similar situation exists when the rotation-vibration perturbations are included. When A and B in Eq. (4), for example, are adjusted in the least

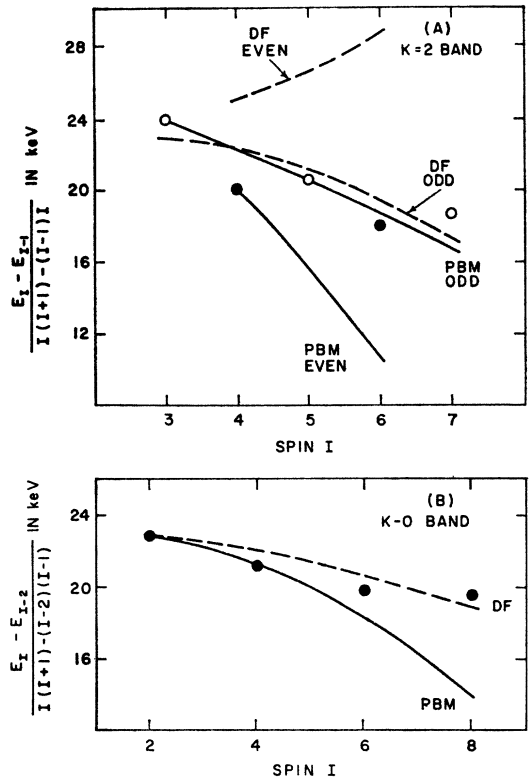

FIG. 11. (A) The experimental points of Fig. 10 are compared with the predictions of the perturbed strong-coupling (PBM) and the asymmetric rotor (DF) models. For the PBM case the adjustable constants have been chosen (as in Table VII, column 5) to fit the four lowest levels of the $K=2$ band. For the DF case, the asymmetry constant, γ, has been chosen to fit the ratio of the energies of 22 and 20 states. While the PBM model predicts that the curves for odd and even spins should diverge as I grows larger, the experimental curves do not diverge. The shift predicted by the DF model (for any $\gamma \neq 0$) is such that the even-I levels are pushed up relative to the odd-I levels. The experimental data show a shift in the opposite direction. (B) A similar plot for energy differences in the ground-state band is shown. The PBM constants have been chosen to fit the 20 and 40 levels, while the DF constants are the same as those in Fig. 11 (A). Each model yields a negative curvature, while the experimental points show a positive curvature.

squares fit, A decreases by 2.8% and B by more than a factor of 2 from the values found from fitting the 2+ and 4+ states (as in Table VII and Fig. 9). Similar changes occur in the parameters for the $K=2$ band.

One may consider the fact that the value of γ found from the ratio of the 2+ energies gives a rather good fit for the energy perturbations in the ground-state bands of the even osmium nuclei to be one of the most important successes of the asymmetric rotor model.

4. Slightly Perturbed Asymmetric Rotor

Following the method of Mallmann and Kerman,[49] one may introduce a first-order rotation-vibration interaction into the asymmetric rotor model by using the relation

$$W(I,"K")=E_0(I,"K")-b[E_0(I,"K")]^2,$$

where $E_0(I,"K")$ is the energy given by the Davydov model for the level of spin I in the "K-band." The parameters γ and b have been adjusted to fit the two 2+ states and the lowest 4+ state of Os^{186}, and the predicted level energies are shown in column 7 of Table VII. The improvement over the unperturbed Davydov model is slight.

Table VIII shows the values of γ and b deduced in this way for those even-mass osmium nuclei for which enough experimental information is available.

TABLE VIII. Values for the parameters γ and b of the slightly perturbed asymmetric rotor model (reference 49) found by fitting the lowest two 2+ states and the lowest 4+ state of some even-A osmium nuclei. The energies are derived from the sources quoted in the caption to Fig. 7.

A	γ	$b\times10^3$
186	16.04°	2.54±0.03
188	18.79°	2.53±0.03
190	21.99°	2.49±0.13
192	25.16°	0.23±0.07

5. Nonadiabatic Asymmetric Rotor

A modification of the asymmetric rotor model which takes into account more exactly the interaction of the rotational motion with the beta-vibrational motion was introduced by Davydov and Chaban.[50] Their parameter μ is essentially a measure of the nonadiabaticity of the rotational motion with respect to the beta vibrations. We have adjusted the parameters of this model to fit the two 2+ states and the lowest 4+ state of Os^{186}, and find $\gamma=15.9°$, $\mu=0.26$. For such a small value of μ the corrections to the level energies may be treated as perturbations, and the predictions of this model are essentially the same as those of the Mallmann-Kerman model (Sec. 4).

6. General Asymmetric Rotor

Mallmann[51] has described a more general asymmetric rotor model, in which the three nuclear moments of inertia are allowed to assume any values, with no restriction by the relations of the hydrodynamic approximation. The rotation-vibration interaction is treated in the same way as in the paper by Mallmann and Kerman. For the level energies, then, there are four parameters: a scale factor; the ratio A/C, which is the ratio of the largest and smallest of the three moments of inertia

[49] C. A. Mallmann and A. K. Kerman, Nucl. Phys. **16**, 105 (1960).

[50] A. S. Davydov and A. A. Chaban, Nucl. Phys. **20**, 499 (1960); E. D. Klema, C. A. Mallmann, and P. Day, Nucl. Phys. **25**, 266 (1961).

[51] C. A. Mallmann, Nucl. Phys. **24**, 535 (1961).

($\vartheta_A = h/4\pi A$, etc.); the quantity κ, defined by

$$\kappa = (2B - A - C)/(A - C);$$

and b, the strength of the rotation-vibration interaction.

We have adjusted the parameters to fit the 2+ and 4+ states of the ground-state band and the 2+ and 3+ states of the $K=2$ band. The parameters are $A/C = 14.612$, $\kappa = -0.7273$, $bE_0(20) = -0.386\%$, and $hC = 12.021$ keV. The corresponding level energies are given in column 8 of Table VII.

Although more parameters are available than in the other asymmetric rotor models, no improvement in the fit is apparent in Table VII.

7. Equality of Intraband Spacing

One prediction in which the strong-coupling and asymmetric rotor models agree is that the energy difference between the first two levels in the $K=2$ band should equal the energy of the first excited state; in other words,

$$E_{32} - E_{22} = E_{20}. \quad (6)$$

The equality may be broken by certain kinds of rotation-vibration interaction or by differences in intrinsic structure. The experimental data for the even osmium nuclei are presented in Table IX. The deviations from Eq. (6) are $\leq 6\%$. It may be noted that their variation with neutron number is not monotonic.

TABLE IX. The energy spacing between the two lowest levels of the $K=2$ band is compared with the spacing between the two lowest levels of the ground-state band. The simple strong coupling and asymmetric rotor models predict that these two spacings should be the same. The percentage deviations from this prediction are given in the last column. The experimental data (except for Os^{186}) are taken from the references given in the caption to Fig. 7.

	$E(20)-E(00)$ (keV)	$E(32)-E(22)$ (keV)	$\frac{E(32)-E(22)}{E(20)-E(00)}-1$
Os^{186}	137.15±0.03	142.95±0.09	(4.23±0.07)%
Os^{188}	155.03±0.03	156.92±0.06	(1.22±0.04)%
Os^{190}	186.7 ±0.1	197.9 ±0.4	(6.0 ±0.2)%
Os^{192}	205.75±0.04	201.31±0.04	(−2.16±0.02)%

8. Summary

In order to have a numerical criterion for the quality of fit of the various models discussed above, a series of least-squares adjustments of the model parameters was performed. The quantity minimized was

$$S^2 = \sum_i \left(\frac{E_{\text{model}}(i)}{E_{\text{exp}}(i)} - 1 \right)^2.$$

Nine levels, the four in the $K=0$ band and five in the $K=2$ band (omitting the less certain 72 level), were included in the sum. The resulting minimum values of S^2, and of the more relevant quantity $S^2/(9-n)$, where n is the number of adjusted model parameters, were calculated. From the results one can say only that most of the models have comparable figures of merit. The strong coupling model with rotation-vibration interaction does give the lowest value for the quantity $S^2/(9-n)$, but in that case the decrease in the number of degrees of freedom renders the result less significant statistically. Finally, it should be noted that, while the rms deviations of these models from the experimental energies range from 1.0% to 3.2%, the rms experimental uncertainty for these same levels is 0.015%.

C. INTERPRETATION OF RELATIVE TRANSITION PROBABILITIES

The relative gamma-ray transition probabilities, as deduced from the intensities given in Table V, for transitions within and between the two collective bands, are now compared with the predictions of the nuclear models discussed in the previous section.[52] For all these transitions except one (that of 143 keV, transition GF) the data either require, or are consistent with, pure $E2$ radiation. We have assumed $E2$ multipolarity also for those transitions within or between the collective bands whose multipolarities have not been determined.

1. Transitions within the Ground-State Band

As an introduction to the discussion of our measurements of relative transition probabilities for transitions from the states in the $K=2$ band, we review briefly the existing information on transitions within the $K=0$ band.

In the strong-coupling model the reduced transition probability from any state in the ground-state band to the next lower state is

$$B(E2; I+2, 0 \rightarrow I, 0) = Q_{00}^2 [C(I+2, 2, I; 000)]^2,$$

where C is a Clebsch-Gordan coefficient and Q_{00} is proportional to the static intrinsic quadrupole moment, Q_0, of the ground state:

$$Q_{00} = (5/16\pi)^{1/2} e Q_0.$$

In first order, the corrections to the collective wave functions introduced by the rotation-vibration interactions of Eqs. (4) and (5) have no effect on the rotational transitions within a band. Similarly, the various versions of the asymmetric rotor model make only small corrections to these transition probabilities.

A summary of determinations of the 20 to 00 transition strength in Os^{186} has been given in Table I. Adopting the value of Bodenstedt *et al.*, which has the smallest uncertainty, one finds $Q_{00} = 1.77e \times 10^{-24}$ cm^2; this corresponds to a deformation, β, of 0.20.

[52] A brief discussion of some of the contents of this section is included in *Electromagnetic Lifetimes and Properties of Nuclear States*, edited by P. H. Stelson, Nuclear Science Series Report No. 37, National Academy of Sciences, National Research Council, Publication 974 (1962), pp. 246–252.

TABLE X. The relative reduced electric quadrupole transition probabilities for transitions from a state in the $K=2$ band to states in the $K=0$ band are compared with the predictions of the strong-coupling, band-mixed strong-coupling, and asymmetric rotor models.

	Experimental ratios	Strong coupling	Band-mixing, $z=0.072$ (or $\gamma\approx12°$)	Asymmetric rotor, $\gamma=16.5°$
$B(E2, 22\rightarrow20)/B(E2, 22\rightarrow00)$	2.1±0.2	1.43	2.16	3.02
$B(E2, 32\rightarrow40)/B(E2, 32\rightarrow20)$	1.0±0.2	0.40	0.96	1.63
$B(E2, 42\rightarrow40)/B(E2, 42\rightarrow20)$	9.3±2.0	2.94	9.40	38.3
$B(E2, 52\rightarrow60)/B(E2, 52\rightarrow40)$	2.3±0.7	0.57	2.31	5.36
$B(E2, 62\rightarrow60)/B(E2, 62\rightarrow40)$	15 ±4	3.71	39.1	340
$B(E2, 72\rightarrow80)/B(E2, 72\rightarrow60)$	(100_{-50}^{+100})[a]	0.67	4.8	25.9

[a] The placement of the 72 level, and the transitions proceeding from it, must be considered tentative.

2. Transitions Between the $K=2$ and $K=0$ Bands

The ratio of reduced transition probabilities, $\mathcal{R}_2 = B(E2, 22\rightarrow20)/B(E2, 22\rightarrow00)$, has been measured for several nuclei. The strong coupling model predicts that $\mathcal{R}_2=10/7$. Experimental values for $\mathcal{R}_2$ are usually slightly larger than 10/7 for strongly deformed nuclei, and the deviations are even larger for nuclei in the transition regions. As mentioned in Sec. IV.A, Van Patter[47] has pointed out that some correlation exists between the experimental values found for these nuclei and the values predicted by the Davydov asymmetric rotor model.

For Os^{186}, a value $\mathcal{R}_2=2.1\pm0.2$ results from our experimental data (see Table X). This value is considerably lower than the asymmetric rotor value 3.02 obtained with $\gamma=16.5°$, which gives the best fit for the level energies. Gregers Hansen, Nielsen, and Sheline[53] have approached the problem of interpreting the experimental data by assuming a certain amount of mixing between the $K=0$ and $K=2$ bands. Following their treatment, let ϵ be defined as the amplitude of admixture of $K=2$ into the wave function of the lowest 2+ state (which is predominantly $K=0$). The admixtures are assumed to be due to a term in the Hamiltonian proportional to $(I_+^2+I_-^2)$, where I_+ (I_-) is the angular momentum operator in the coordinate system fixed in the nucleus which lowers (raises) K by one unit. The amplitude of admixture in the higher even-spin states is then

$$(\text{Amplitude})_I=[(I-1)I(I+1)(I+2)/24]^{1/2}\epsilon. \quad (7)$$

Let Q_{20} be defined as the reduced $E2$ matrix element for transitions with $|\Delta K|=2$. Without band mixing one would have

$$B(E2, I'2\rightarrow I0)=Q_{20}^2[C(I'2I; 2, -2, 0)]^2.$$

Since transitions within a band are, in general, more enhanced than transitions between bands, one expects that Q_{20} is smaller than Q_{00}. Now let

$$z=\epsilon Q_{00}/Q_{20}. \quad (8)$$

The effects of the band mixing on the $I'2\rightarrow I0$ transitions are then expressed by a function $f_{I'I}(z)$, which is the square of a function linear in z. The ratio $\mathcal{R}_2$ becomes, with band mixing,

$$\mathcal{R}_2=\frac{10}{7}\left(\frac{1+2z}{1-z}\right)^2. \quad (9)$$

A table of the function $f_{I'I}(z)$ was published by Gregers Hansen, Nielsen, and Sheline,[53] and was included in a review article by Sheline.[54] An analysis of data for several nuclei in terms of this kind of band mixing has been presented by Nielsen.[55]

For Os^{186}, one finds that the value $z=0.072$ fits the experimentally determined ratios $\mathcal{R}_I$ for $I=2$, 3, 4, and 5. The experimental results are given in column 2 of Table X; the strong-coupling predictions ($z=0$) are given in column 3; and the ratios including the band-mixing factors $f_{I'I}(z)$, with $z=0.072$, are given in column 4.

The Davydov asymmetric rotor model also gives predictions for these ratios of between-band transition probabilities. The ratio $\mathcal{R}_2$, for example, is given by

$$\mathcal{R}_2=\frac{10}{7}\frac{2\sin^2 3\gamma}{(9-8\sin^2 3\gamma)^{1/2}[(9-8\sin^2 3\gamma)^{1/2}-(3-2\sin^2 3\gamma)]}.$$

If one expands this expression in powers of γ, one finds

$$\mathcal{R}_2=(10/7)[1+8\gamma^2+O(\gamma^4)], \quad (10)$$

where $O(\gamma^4)$ denotes a term of order γ^4. It is clear from the comparison of Eqs. (9) and (10) that, for small γ and z, the two models are mathematically equivalent in their predictions for $\mathcal{R}_2$, and that the two parameters are related by the equation

$$z=\tfrac{4}{3}\gamma^2. \quad (11)$$

It is now shown that this correspondence holds for all ratios $\mathcal{R}_I$, that is, for all ratios of reduced transition

[53] P. Gregers Hansen, O. B. Nielsen, and R. K. Sheline, Nucl. Phys. **12**, 413 (1959).

[54] R. K. Sheline, Rev. Mod. Phys. **32**, 1 (1960).

[55] O. B. Nielsen, in *Proceedings of the Rutherford Jubilee Conference, Manchester, 1961* (Academic Press Inc., New York, 1961), p. 317.

probabilities for $E2$ transitions from any state I in the $K=2$ band to any two states in the ground-state band. The amplitude of admixture in the Davydov model, for small γ, is $[(I-1)I(I+1)(I+2)/24]^{1/2}\times(4/3)\gamma^3$. If one compares this expression with that given in Eq. (7), one sees that the two expressions are equivalent for

$$\epsilon=\tfrac{4}{3}\gamma^3. \tag{12}$$

In the band-mixing model, the $\Delta K=2$ transition amplitudes are of the form $Q_{20}C(I'2I;2,-2,0)$ and the $\Delta K=0$ amplitudes are $Q_{00}C(I'2I;KOK)$. The ratio Q_{00}/Q_{20} is replaced in the Davydov model by $\cot\gamma$ or, for small γ, by γ^{-1}. Substituting this value for Q_{00}/Q_{20} and the expression for ϵ [Eq. (12)] in the definition of z [Eq. (8)], we arrive at the result shown in Eq. (11). A value for z of 0.072 corresponds to a value for γ of about 12°, as indicated at the top of column 4 of Table X.[56]

As shown in Sec. B.3, the value of γ deduced from the Os^{186} level energies is 16.5°. The asymmetric rotor transition probability ratios for this value of γ are given in column 5 of Table X. Clearly, different values of γ are required to fit these two different classes of data. Thus, for all the known $K=2$ levels in Os^{186} there is a systematic deviation from the asymmetric rotor transition probability predictions, which should be kept in mind in evaluating the approximate correlation for the $\mathcal{R}_2$ values noted by Van Patter. In Table XI, the values of γ required by the energy ratios (γ_E) are compared with those required by the between-band transition probability ratios (γ_{TP}) for four even osmium isotopes. The discrepancy between the two quantities is smaller for the heavier isotopes.

TABLE XI. Comparison of values for the asymmetric rotor parameter, γ, found for osmium isotopes from energy ratios with those found from electric quadrupole transition probability ratios. γ_E is taken from the energy ratio of the lowest two 2+ states, and γ_{TP} is taken from the ratio $\mathcal{R}_2$, defined in the text. The experimental data for isotopes other than Os^{186} are taken from the references given in the caption to Fig. 7.

A	γ_E	γ_{TP}	$\Delta\gamma$
186	16.51±0.01°	12.0±1.2°	4.5±1.2°
188	19.16±0.03°	15.6±0.5°	3.6±0.5°
190	22.29±0.03°	20.8±0.8°	1.5±0.8°
192	25.19±0.02°	23.2±0.6°	2.0±0.6°

In a perturbation theory approximation which includes only first order corrections to the wave functions, the general asymmetric rotor model of Mallmann is completely equivalent to the two descriptions discussed above for between-band transition probability ratios. The expansion of the wave functions in terms of eigenstates of K, and thus the amount of admixture, ϵ, is determined solely by the parameter κ. Mallmann also introduces the parameter r, which is defined as Q_{20}/Q_{00}. One can fit the ratios of between-band transition probabilities with any combination of r and κ such that $z=\epsilon(\kappa)/r=0.072$; therefore with any such choice of parameters the predicted ratios $\mathcal{R}_I$ are those given in column 4 of Table X.

3. Relative Strengths of Rotational and Vibrational Transitions

There is a second class of relative transition probabilities which may be considered, consisting of cases in which a transition within the $K=2$ band is compared with one from the $K=2$ band to the $K=0$ band. In the strong coupling model such ratios of reduced transition probabilities are directly proportional to $(Q_{00}/Q_{20})^2$. When band mixing is taken into account, the $B(E2)$ value for the between-band transition must be multiplied by the appropriate factor $f_{I'I}(z)$; this correction is not negligible. Table XII shows four such experimental ratios. They are compared with the band-mixed strong coupling predictions, with $z=0.072$, as determined before. The best fit with the experimental ratios is obtained for $(Q_{00}/Q_{20})^2\approx 10$. The ratio $(Q_{00}/Q_{20})^2$ can, in general, also be determined from the ratio of the $B(E2)$ values obtained by Coulomb excitation of the first and second 2+ states. This measurement has not yet been made for Os^{186}, because of the low natural abundance of this isotope, but it is interesting to compare the value obtained here from the analysis of the transition probabilities with the values obtained from

TABLE XII. Ratios of reduced transition probabilities from levels in the $K=2$ band. For each level a transition within the $K=2$ band is compared with one to the $K=0$ band.

	Experimental ratios	Band-mixed strong coupling, $(Q_{00}/Q_{20})^2=10$, $z=0.072$	Asymmetric rotor $\gamma=16.5°$	Asymmetric rotor $\gamma=12°$
$B(E2,42\to22)/B(E2,42\to20)$	33.5±8.4	24	96	49
$B(E2,52\to32)/B(E2,52\to40)$	6.2±1.6	10	20	21
$B(E2,62\to42)/B(E2,62\to60)$	6.2±1.2	5.0	6.1	11
$B(E2,72\to62)/B(E2,72\to80)$	(4_{-2}^{+4})[a]	1.8	1.9	3.8

[a] The placement of the 72 level, and the transitions proceeding from it, must be considered tentative.

[56] That there is a correspondence between the two models in their predictions concerning these ratios of between-band transition probabilities was noted by G. T. Ewan, R. L. Graham, and J. S. Geiger, Nucl. Phys. 22, 610 (1961).

TABLE XIII. The ratio $(Q_{00}/Q_{20})^2$ found in this work for Os^{186} is compared with the same quantity for other osmium nuclei deduced from the results of McGowan and Stelson (reference 46), who measured the reduced transition probabilities, $B(E2, 00 \rightarrow IK)$, for Coulomb excitation of the 20 and 22 states. The band-mixing correction, $(1-z)^2$, for the $00 \rightarrow 22$ transition, has been applied, using the z values shown; these z values are derived from analysis of between-band transition probability ratios (Sec. C.2). The quantity γ_Q is defined by $\cot^2\gamma_Q = (Q_{00}/Q_{20})^2$; the results for γ_Q are consistent with either γ_E or γ_{TP} in Table XI, except for Os^{186}, where γ_Q is consistent only with γ_E.

Nucleus	$B(E2, 00 \rightarrow 22)/B(E2, 00 \rightarrow 20)$	z	$(Q_{00}/Q_{20})^2$	γ_Q
Os^{186}	...	0.072±0.010[a]	10 ±3	18.4±3.2°
Os^{188}	0.070±0.022	0.12 ±0.01[b]	11.0±3.5	16.7±2.6°
Os^{190}	0.071±0.017	0.27 ±0.04[c]	7.5±2.0	20.1±2.4°
Os^{192}	0.103±0.022	0.34 ±0.08[d]	4.1±1.4	26.1±3.9°

[a] This work.
[b] Reference 29.
[c] Computed from the data of reference 2.
[d] Computed from the data of reference 46.

Coulomb excitation of Os^{188}, Os^{190}, and Os^{192} by McGowan and Stelson.[46]

The ratios of $B(E2)$ for the excitation of the two 2+ states, and the resulting quantities $(Q_{00}/Q_{20})^2$, are shown in Table XIII for four neighboring even-mass osmium isotopes. Also shown are values of γ_Q, defined by $\cot^2\gamma_Q = (Q_{00}/Q_{20})^2$. It is interesting to note that γ_Q agrees within limits of error with either γ_E or γ_{TP} (see Table XI) except for the case of Os^{186}, where it agrees only with γ_E.

With (Q_{00}/Q_{20}) thus fixed as approximately 3.1, the parameter of admixture, ϵ, must be approximately 0.023, according to Eq. (8). It has been pointed out by Nielsen[55] that this amount of admixture is not nearly large enough to explain the large deviations from the $I(I+1)$ energy spacing found in the ground-state band of Os^{186}, and that a similar situation exists for each of the other deformed nuclei for which sufficient data are available to carry out this kind of analysis.

The asymmetric rotor theories also make predictions for this class of transition probability ratio. The results for the Davydov hydrodynamic version, for the two values of γ discussed earlier, are shown in Table XII; no value of γ fits the experimental results. The Mallmann model and the band-mixing model are equivalent for the description of these transition probability ratios also, in the parameter range needed for the description of deformed nuclei; thus the Mallmann model will fit the experimental results for $r^{-1} = (Q_{00}/Q_{20}) \approx 3.1$ and $z = r^{-1}\epsilon(\kappa) \approx 0.072$. These values of z and r imply $\kappa = -0.90$, a value significantly different from the value -0.73 found from analysis of the level energies.

D. SPINS OF EVEN MASS IRIDIUM AND RHENIUM NUCLEI

In the course of this work it was concluded that the ground-state spin and parity of Ir^{186} are probably 7−. It is interesting to speculate on the probable configuration of this state and also of the ground states and excited states of some other even-A iridium nuclei and rhenium nuclei, whose characters have recently been determined.

Since no direct determinations of the ground-state spins of these nuclei have been carried out so far, our information is based entirely on the decay characteristics of these states. Table XIV summarizes the experimental evidence.

TABLE XIV. Summary of experimentally determined ground-state spins and parities of even A rhenium and iridium nuclei. Spins and parities of some isomeric states are also listed.

Nuclide	N	Energy of state (MeV)	Half-life	$I\pi$	Reference
Re^{186}	111	0	90 h	1−	a
Ir^{186}	109	0	15.8 h	7(−)	b
Re^{188}	113	0	17 h	1−	c
Ir^{188}	111	0	41 h	2−	c
Re^{190}	115	0	2.8 min	(3−)	c
Ir^{190}	113	0	12.3 day	4−	d
Ir^{190m}		≈2.5	3.2 h	9, 10, 11−	e
Ir^{192}	115	0	74 day	4±	f
Ir^{192m_1}		0.058	1.4 min	1∓	f
Ir^{192m_2}		0.131	650 yr[g]	9∓	f

[a] Porter, Freedman, Novey, and Wagner, reference 6.
[b] Present work.
[c] *Nuclear Data Sheets*, National Academy of Sciences, National Research Council (U. S. Government Printing Office, Washington 25, D. C., 1959).
[d] Kane, Emery, Scharff-Goldhaber, and McKeown, reference 2.
[e] G. Scharff-Goldhaber, D. E. Alburger, G. Harbottle, and M. McKeown, Phys. Rev. 111, 913 (1958); and private communication.
[f] Scharff-Goldhaber and McKeown, reference 59.
[g] G. Harbottle, Nucl. Phys. (to be published).

It is interesting to examine this evidence in the light of the recent study of the coupling of angular momenta in odd-odd nuclei by Gallagher and Moszkowski[57] and by Gallagher and Soloviev.[58] The ground-state characters of the odd-mass Re and Ir nuclei appear to be uniformly $5/2+[402\uparrow]$ and $3/2+[402\downarrow]$ respectively, and from the odd-A osmium isotopes we can infer information on the neutron orbitals as shown in Table XV.

Table XVI represents an attempt to interpret the spins and parities of the even-mass Re and Ir nuclei listed in Table XIV by applying the coupling rules proposed by Gallagher and Moszkowski.[57] Where it is possible to represent the observed character on the basis of these coupling rules and orbital assignments,

[57] C. J. Gallagher, Jr., and S. A. Moszkowski, Phys. Rev. 111, 1282 (1958).
[58] C. J. Gallagher, Jr., and V. G. Soloviev, Kgl. Danske Videnskab. Selskab, Mat.-Fys. Skr. 2, No. 2 (1962).

TABLE XV. Experimental ground-state spins and parities of wolfram and osmium isotopes with odd neutron number. Addition of a proton to each of these nuclei results in the rhenium and iridium isotopes listed in Table XIV. The most probable Nilsson orbital is added in square brackets.

N	A(W)	I π	Assigned[a] orbital	Reference	A(Os)	I π	Assigned[a] orbital	Reference
109	183	1/2 −	[510↑]	b	185	1/2 −	[510↑]	b
111	185	3/2 −	[512↓]	b	187	1/2 −	[510↑]	b
113	187	3/2 −	[512↓]	b, c	189	3/2 −	[512↓]	b
115	189		?		191	(9/2) −	[505↓]	b

[a] The notation used here for the identification of the ground states is that used by B. R. Mottelson and S. G. Nilsson, Kgl. Danske Videnskab. Selskab, Mat.-Fys. Skr. 1, No. 8 (1959). The arrow indicates the direction of the intrinsic spin of the neutron relative to its orbital angular momentum (↑ parallel, ↓ antiparallel).
[b] *Nuclear Data Sheets*, National Academy of Sciences, National Research Council (U. S. Government Printing Office, Washington 25, D. C., 1959).
[c] W. M. Doyle and R. Marrus, Bull. Am. Phys. Soc. 7, 476 (1962).

column 5 states "Yes"; where this is not possible and other Nilsson orbitals have to be invoked, column 5 states "No."

It appears that the coupling rules discussed above are compatible with the results on the Re nuclei, whereas they do not apply to the Ir nuclei. The analysis given in Table XVI further suggests that the parities of the triple isomers of Ir^{192}, which have so far been ambiguous,[59] are probably (4)+, (1)−, (9)−.

A detailed study of the interpretation, in terms of Nilsson orbitals, of the states listed above should provide valuable information on the interactions between the odd protons and the odd neutrons in this transition region from the spheroidal to the spherical shape.

E. OSMIUM-IRIDIUM MASS DIFFERENCES

The total disintegration energies of the even-A iridium isotopes are shown in Fig. 12. For comparison

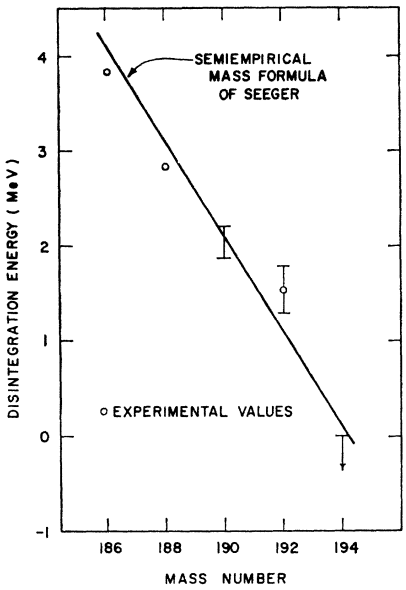

FIG. 12. A comparison of even-A iridium-osmium total disintegration energies with values predicted by the semiempirical mass formula of Seeger (reference 60). Empirical disintegration energies were arrived at from the following sources: Ir^{186}: From the present work, $Q_{ec}=3.83\pm0.02$ MeV. Ir^{188}: L. B. Warner and R. K. Sheline, Nucl. Phys. **36**, 207 (1962), $Q_{ec}=2.83\pm0.01$ MeV. Ir^{190}: reference 2, $1.88\leq Q_{ec}\leq 2.20$ MeV. Ir^{192}: From the $Ir^{192}\rightarrow Pt^{192}$ disintegration energy given in *Nuclear Data Sheets* and the mass difference between Pt^{192} and Os^{192} as measured by R. A. Demirkhanov, T. I. Gutkin, and V. V. Dorokhov, Zh. Eksperim. i Teor. Fiz. **37**, 1217 (1959) [translation: Soviet Phys.—JETP **10**, 866 (1960)], the value $Q_{ec}=1.54\pm0.25$ MeV has been derived for the $Ir^{192}\rightarrow Os^{192}$ decay. If the weak positron branch ($E_{\beta+}=0.24\pm0.01$ MeV) reported for Ir^{192} by Antonova, Vasilienko, Kagansky, and Kaminsky (reference 62) is assumed to populate the 206-keV level of Os^{192}, then $Q_{ec}=1.47\pm0.01$ MeV. Ir^{194}: From the nonoccurrence of Os^{194} in nature, $Q_{ec}\leq 0$ for Ir^{194}.

TABLE XVI. Possible configurations of Nilsson orbitals resulting in the spins and parities of the rhenium and iridium nuclei listed in Table XIV. Column 4 gives the ground-state angular momentum of the odd neutron in the nucleus $(Z-1, N)$ and of the odd proton in the nucleus $(Z, N-1)$. Where it is possible to interpret the experimentally determined nuclear spins as due to the coupling of such a "ground-state" neutron and proton with their intrinsic spins lined up in the same direction, Column 5 states "yes"; where this is not possible, it states "no."

(1)	(2) Expt $I\pi$	(3) Possible configuration p	(3) Possible configuration n	(4) Ground-state spins in odd-A nuclei p	(4) Ground-state spins in odd-A nuclei n	(5)
Re^{186}	1−	[402↑]5/2+	[512↓]3/2−	5/2+	3/2−	Yes
Ir^{186}	7(−)	[404↓]7/2+	[514↓]7/2−	3/2+	1/2−	No
Re^{188}	1−	[402↑]5/2+	[512↓]3/2−	5/2+	3/2−	Yes
Ir^{188}	2−	[402↓]3/2+	[503↑]7/2−	3/2+	1/2−	No
Re^{190}	(3−)	[402↑]5/2+	[510↑]1/2−	5/2+	?	
Ir^{190}	4− or	[400↑]1/2+ [400↑]1/2+	[503↑]7/2− [505↓]9/2−	3/2+	3/2−	No
Ir^{190m}	9, 10, 11−	[514↑]9/2− [505↑]11/2−	[615↑]11/2+ [624↑]9/2+ → 10−			
		[514↑]9/2− [505↑]11/2−	[624↑]9/2+ [615↑]11/2+ → 9− 11−			
Ir^{192}	4±	[505↑]11/2−	[512↓]3/2− → 4+	3/2+	9/2−	No
Ir^{192m_1}	1∓ or	[400↑]1/2+ [400↑]1/2+	[510↑]1/2− [512↓]3/2− → 1−			
Ir^{192m_2}	9∓	[514↑]9/2−	[624↑]9/2+ → 9−			

[59] G. Scharff-Goldhaber and M. McKeown, Phys. Rev. Letters **3**, 47 (1959).

the values predicted by the semiempirical mass formula of Seeger[60] are also shown. The origins of the experimental disintegration energies are given in the caption to Fig. 12. With the exception of Ir^{192}, the experimental values are seen to exhibit the usual linear dependence on mass number.[61] For Ir^{192}, the total disintegration energy expected from an interpolation of the other experimental points falls below 1 MeV. However, both the reported 0.24-MeV positron branch[62] in the decay of Ir^{192}, and the disintegration energy computed from mass differences (caption to Fig. 12) yield a disintegration energy of $\sim$1.5 MeV.

F. SUMMARY AND CONCLUSIONS

A comparison of the level scheme of Os^{186} with the level schemes of neighboring even-A osmium nuclei shows that it represents one step in a gradual transition from level schemes resembling those of strongly deformed nuclei to schemes of a near-harmonic nature (see Figs. 7 and 8). In addition to the deviations from the strong coupling predictions which are apparent in Figs. 8 and 9, there is found an odd-even shift in the $K=2$ band, such that the levels of even spin ($I=2$, 4, 6) are shifted downward with respect to the levels of odd spin ($I=3$, 5, 7). An attempt to fit the levels of the ground-state band by the introduction of rotation-vibration perturbations [an $I^2(I+1)^2$ term] leads to negative deviations of the predicted 6+ and 8+ levels of the same order of magnitude as the positive deviations obtained from the strict strong coupling formula (see Fig. 9; the same point is shown in a different way in Figs. 10 (B) and 11 (B), where the experimental curve shows a positive curvature, while the rotation-vibration term gives a negative curvature to the PBM curve). Corrections of the same order for the $K=2$ band include a term which affects only the levels of even spin, but it is proportional to $[I^2(I+1)^2-2I(I+1)]$, while the experimental shift seems not to be proportional to such a high power of I; that is, the experimental curves for odd and for even spin [Fig. 10(A)] seem to show an almost constant difference, while the rotation-vibration odd-even term [Fig. 11 (A)] predicts odd and even curves whose difference is proportional to (approximately) I^2.

The asymmetric rotor model of Davydov and Filippov fits the level energies remarkably well, with the exception of the two highest levels of the $K=2$ band (Fig. 9). This model, however, predicts that the even-I levels of the $K=2$ band should be raised relative to the odd-I levels, while the experimental odd-even shift is in the opposite direction. More complicated asymmetric rotor models do not improve the fit to the level scheme.

Analysis of relative transition probabilities for collective $E2$ transitions shows agreement with the band-mixing approach (Tables X and XII). The Davydov model can fit ratios of between-band transition probabilities, but with a value of γ different from that which fits the energies. It is shown that if such ratios of between-band transition probabilities can be fitted by the band-mixing approach with a small value of z, they can equally well be fitted by the Davydov model with a value of γ such that $z=(4/3)\gamma^2$. The Davydov model does not fit ratios of between-band to in-band transition probabilities. The general asymmetric rotor model of Mallmann can fit both types of ratios, but, for the parameter values required, it is equivalent to the band-mixing approach. If one uses either the general asymmetric rotor model or the band-mixing approach, the amount of mixing between the $K=2$ and $K=0$ bands necessary to fit simultaneously both kinds of transition probability ratios is not large enough to account for the large energy deviations in the $K=0$ band from the normal $I(I+1)$ dependence. From the analysis of between-band to in-band transition probability ratios one derives the ratio of the rotational and vibrational transition quadrupole moments; this ratio for Os^{186} is consistent with those found for higher mass osmium nuclei from Coulomb excitation, which show a smooth decrease with mass number (Table XIII).

An attempt to interpret the ground-state spins of the odd-odd iridium and rhenium isotopes in terms of the Nilsson model is only partly successful.

Even-A iridium-osmium mass differences show a consistent pattern, and agree fairly well with the results of current semiempirical mass formulas.

ACKNOWLEDGMENTS

We are greatly indebted to C. P. Baker for arranging the α-particle bombardments of the rhenium targets inside the 60-in. cyclotron. Elizabeth W. Baker deserves our thanks for her able assistance in preparation of the rhenium targets and separation of the iridium activity. We also wish to thank M. Schmorak for following the decay of the high-energy gamma rays, and N. F. Fiebiger for the loan of the 64×32 channel pulse-height analyzer and the three-crystal pair spectrometer.

For the analysis of the data we received the valuable help of two members of the Mathematics Division: K. Fuchel and L. Lawrence.

The great stability and accuracy of the double-focusing spectrometer is to a very large extent due to the ingenious design of the auxiliary equipment by R. Chase. E. Bindel was very helpful in setting up the spectrometer.

We were encouraged to carry out this research on the basis of the results of earlier studies of the γ rays, the conversion-electron lines, and the positron spectrum, which were carried out by D. E. Alburger in collaboration with two of the present authors (G. S.-G. and M. McK.) during the years 1957 and 1958. The sources for this early work were prepared by G. Harbottle and,

[60] P. A. Seeger, Nucl. Phys. **25**, 1 (1961).
[61] K. Way and M. Wood, Phys. Rev. **94**, 119 (1954).
[62] S. F. Antonova, S. S. Vasilienko, M. G. Kagansky, and P. L. Kaminsky, Zh. Eksperim. i Teor. Fiz. **38**, 379 (1960) [translation: Soviet Phys.—JETP **11**, 276 (1960)].

later, by J. Hudis; their resourcefulness and unflagging enthusiasm proved to be very stimulating.

Don S. Harmer kindly furnished, before publication, some results of his calculations of screened, finite-size, positron wave functions, which were used in the analysis of the positron spectrum.

It is a pleasure to acknowledge many fruitful discussions with J. Weneser concerning the theoretical aspects of this work.

APPENDIX I

In the course of the study of the internal conversion-electron spectra of Ir^{186}, data were obtained also on transitions which occur in the decay of Ir^{185} and Ir^{187}. These are presented in Tables XVII and XVIII together with data obtained on some of these transitions by Diamond and Hollander.[21] The study of these isotopes is being continued.[63]

TABLE XVII. Transitions observed in the decay of Ir^{185}. Intensities given in the second column are for the conversion lines there designated, and $6.2(-1)$ is to be read as 6.2×10^{-1}; observed peak counting rates were approximately 10^5/min multiplied by the number given.

E_γ (keV)	Conversion line intensity	Conversion lines observed, basis of multipole assignment, remarks	Values of Diamond and Hollander[a] E_γ	Mass assignment
59.89±0.10	~1(−1)M	M.	59.9	185
90.18±0.26	~2(−1)L_3	L_1, L_3, M.	92.7 or 153.6	185
97.15±0.27	6.2(−1)L_2	L_2, L_3, M. $L_2/L_3/M=(6.2\pm0.8)/(5.0\pm0.8)/(2.7\pm0.4)$. $E2$.	97.3	185
100.09±0.54	~8(−2)M	L_2, M.	100.8	185
139.14±0.15	8.2(−2)K	K.		
254.16±0.11	3.2(−1)K	K, L_1, M. No L_3. Not $E2$.	254.4	185
274.37±0.18	~3(−3)K	K.		
445.95±0.28	~6(−2)K	K.		
451.38±0.64	~3(−3)K	K?		
489.05±0.20	3.5(−2)K	K.		
513.98±0.67	~1(−2)K	K.		
666.85±0.71	~8(−3)K	K.		

[a] Reference 21.

TABLE XVIII. Transitions observed in the decay of Ir^{187}. Refer to caption of Table XVII for interpretation of data in second column.

E_γ (keV)	Conversion line intensity	Conversion lines observed, basis of multipole assignment, remarks	Values of Diamond and Hollander[a] E_γ (keV)	Mass assignment
65.15±0.15	1.3(0)L_3	L_2, L_3. No L_1; not $E1$. $L_2/L_3=0.7\pm0.2$. $E2$.	65.2	187
73.67±0.10	2.9(−1)L_2	L_2, M. L_3 hidden.	74.2	187
85.00±0.07	1.9(−1)L_1	L_1, M. No L_2 or L_3; not $E2$.		
125.52±0.06		K, L. Both lines are complex.		
137.91±0.12		K. Weak.		
162.59±0.21	2.5(−2)K	K.	162.9	186 or 187
177.49±0.11	2.8(−1)K	K, $L_{1,2}$, L_3. $K/L_{1,2}/L_3=(2.9\pm0.1)/(0.57\pm0.02)/(0.029\pm0.005)$. $M1+E2$.	177.6	187
187.08±0.15	6.0(−2)K	K, $L_{1,2}$, L_3, M. $K/L_{1,2}/L_3/M=(6.0\pm0.2)/(3.3\pm0.1)/(1.5\pm0.1)/(1.8\pm0.1)$. $E2$.	187.5	187
313.83±0.12	2.9(−2)K	K, $L_{1,2}$, M.	314.0	187
399.22±0.23	4(−3)K	K.		
400.85±0.15	2.1(−2)K	K, $L_{1,2}$, M.	401.0	187
426.92±0.14	5.6(−2)K	K, $L_{1,2}$.	427.2	187
491.14±0.25		K. Weak		
501.50±0.17	1.5(−2)K	K, L_1.	502	prob. 186 or 187
576.47±0.39	4(−3)K	K.	577	
610.59±0.37	2.2(−2)K	K, $L_{1,2}$.	612	prob. 186 or 187
799.36±0.73	3(−3)K	K.		
912.59±0.42	1(−2)K	K.	914	prob. 187
976.74±0.50	4(−3)K	K.	979	prob. 187
987.03±0.43	5(−3)K	K.	990	prob. 187

[a] Reference 21.

[63] A recent paper by B. Harmatz, T. H. Handley, and J. W. Mihelich [Phys. Rev. 128, 1186 (1962)] contains information on the decay of Ir^{185} and Ir^{187}, as well as on other decays. We thank these authors for informing us of this work.

APPENDIX II

In the construction of the level scheme with the use of energy sums there are evidently a large number of chance relationships. Because the measured transition energies have average uncertainties of ~0.5 keV and there are ~5000 energy sums in the interval 150–3600 keV, the probability that there will be a chance agreement of at least one energy sum with the energy of a given transition is close to unity. Accordingly, it is necessary to consider the probability that some of the levels so established may be spurious.

The problem is that of fitting a number of transitions into a level scheme in which most individual levels, on various grounds, have a very small probability of being spurious.[64] The search for new levels is made by taking each transition in turn, supposing that it populates a given, already established level (thus postulating a new level with energy $E_{\text{level}}+E_{\text{transition}}$), and determining if other transitions connect the postulated level with other, established levels. For each transition this process is repeated for all possible locations in the level scheme, i.e., populating all established levels. Possible new levels so established which were connected by $n=4$ or more transitions to other levels were considered for inclusion in the final level scheme.

For a trial fit of one transition to one already established level, the probability of $n-1$ chance connections to $n-1$ other levels out of N levels is given by the binomial distribution

$$P_n=\binom{N-1}{n-1}p^{n-1}(1-p)^{N-n},$$

where $\binom{N-1}{n-1}$ is the binomial coefficient and p is the average probability of a single chance connection with another level. Here N, the total number of levels, is slightly smaller than the total number in the level scheme because transitions at very low and very high energy were not observed, and hence were not available for trial fits to certain levels, so that $N\sim 20$. From the average energy spacing of the transitions to be fitted and their estimated errors the probability p of a single false connection is ~0.04. Hence, for $n=4$,

$$P_4=\binom{19}{3}(0.04)^3(0.96)^{16}\approx 3\times 10^{-2}.$$

In the process of attempting to fit a given transition into all possible locations in the level scheme the probability of occurrence of a spurious level (for $n=4$) is given by a second, similar binomial distribution involving P_4. Since P_4 is small, this probability may be approximated by NP_4. Here

$$NP_4\approx 0.6.$$

Finally the expected number of spurious levels would be NP_4 times the number of transitions to be fitted, except for the fact that in the search fourfold fits are counted four times. There are approximately 50 transitions to be fitted, so the expected number of spurious levels connected to other levels by $n=4$ transitions is

$$(50\times 0.6/4)\approx 8.$$

Those cases in which a transition occurs more than once must be examined, and one must reject all but one of the fourfold fits including that transition. One can estimate that the number of spurious levels rejected by this process is ~4; thus the number of spurious levels remaining to be examined in the light of additional experimental evidence is ~4.

[64] This is not identical with the problem of attempting to construct a level scheme from a table of transition energies in the absence of any other information about the level scheme.